International Journal of Biomathematics
(2024) 2450068 (33 pages)

DOI: 10.1142/S1793524524500682

How can we avoid the extinction of any species naturally? A mathematical model

A. K. Misra* and Soumitra Pal†

Department of Mathematics, Institute of Science
Banaras Hindu University, Varanasi 221005, India
**akmisra_knp@yahoo.com*
†*soumitrapal8@gmail.com*

Yun Kang

Science and Mathematics Faculty
College of Integrative Sciences and Arts
Arizona State University, Mesa, AZ 85212, USA
yun.kang@asu.edu

Received 18 September 2023
Revised 3 May 2024
Accepted 25 May 2024
Published 10 July 2024

Communicated by Bing Liu

A large number of herbivorous mammals and reptiles in many terrestrial ecosystems across the globe are presently in the receiving end of extinction. Over-exploitation by its immediate predator and anthropogenic actions is one of the main reasons. Reintroduction of apex predator or top predator at some instances has proven to be a successful strategy in restoring ecological balance. In this paper, we conceptualize the role of top predator in enriching the density of vulnerable species of lower trophic level, with the help of mathematical modeling. First, the dynamical behavior of two species system (prey and mesopredator) is studied, where growth of prey is subject to strong Allee effect. Also, the cost of predation induced fear is incorporated in the growth term. Parametric regions, for which the species perceive extinction risk are analyzed and depicted numerically. We consider that whenever density of the vulnerable species reach a certain threshold, minimum viable population, top predator is introduced in the habitat. Our obtained results show that a species population can be restored from the verge of extinction to a stable state with much higher population density with the introduction of top predator and even it stabilizes an oscillatory system.

Keywords: Top predator; fear effect; Allee effect; ratio-dependent functional response; extinction; bifurcations.

*Corresponding author.

1. Introduction

Species extinction rate is unprecedentedly growing over time. According to the International Union of Conservation of Nature (IUCN), 160 species have gone extinct in the last decade [1], which includes mammals, reptiles, birds and plants. Furthermore, 18% of extant vertebrates have been declared vulnerable [2]. Atwood *et al.* [7] concluded from their study that herbivores perceive elevated predation risk among mammals, birds and reptiles. Some theoretical studies with the help of mathematical modeling have been done to preserve endangered species. Oliveira and Hilker [32] explored bio-control approach by introducing disease in invasive predator species. Disease weakens the predators and the augmented death results in limiting the predation, which in turn will allow the endangered species to recover. Numfor *et al.* [31] studied optimal control strategy of trapping and culling of invasive predators along with bio-control strategy to conserve endangered species. As every organism has fair contribution and specific role in shaping and preserving the healthy ecosystems in which they dwell, continuous species loss has influenced the ecology of our planet profoundly. All the species in terrestrial or aquatic ecosystem occupy some trophic level in the food chain. Often, extinction of lower trophic species leads to secondary extinction. Predation or feeding serves as the bridge between trophic levels, which provides the pathway for energy to flow from lower trophic levels to higher trophic levels. The entire idea of energy flow mechanism is based on the bottom-up approach, i.e. the cumulative resources, like food and habitat available for lower trophic level ultimately determine the fate of those species occupying higher trophic levels. This concept of bottom-up approach has been considered as one of the main tenets of ecology. However, to answer the famous question "why is the Earth green?", ecologists agreed that influence of top-down approach along with bottom-up approach is also pervasive [20, 38]. In this top-down approach, the role of predators becomes significant in shaping the ecosystem. Carnivores weeding out weak, slow and dying animals, which belong to their prey community, and thus keep prey population in check. The presence of predators restrains herbivores from accessing and over-utilizing the plant resources they feed upon. Thus, predation is not only beneficial for predators, but also keeps the entire ecosystem healthy. Therefore, ecologists come out with the concept of introducing top predator as one of the most plausible techniques to improve ecological functioning. Sergio *et al.* [44] reviewed the role of top predators in bio-diversity restoration in reference of various ecosystems. Baker *et al.* [8] proposed an ensemble modeling method to study the potential outcomes of keystone predator reintroduction in an ecosystem.

An experiment of repatriation of wolf in Yellowstone national park in the USA comes out with resounding success in reviving the degrading ecosystem. In 1995, eight wolves were reintroduced in Yellowstone national park with the expectation of restoring the continuously deteriorating ecosystem. Reintroduction of wolves brought back lots of ecological benefits for the whole national park ecosystem [39]. As predation by wolves limits the population of deer and elk, some endangered

plant species were observed in more patches, colony of beaver species increased, more songbirds were being observed as canopy increased, more scavengers were seen as carcasses increased. Some barren land came to life as grazing decreased by some amount. Besides that, more interestingly, it is observed that the behavior and grazing pattern of elk have changed in the presence of wolves. Very recently, in 2018, the reintroduction of wolves in Isle Royale Island also got reverberating success in bringing back the degrading ecosystem to its healthy state [48].

Mathematical modeling provides a platform to understand the dynamic process involved in ecology and are often useful to make practical predictions and derive insightful conclusions. Starting from the seminal work of Lotka–Volterra [30, 54], theoretical study of predator–prey interaction and food web system traverse a long way with the help of mathematical modeling and has proven to be a persuasive alternative for time consuming and often risky field experiments. Development of mathematical models with the incorporation of species specific traits engaged many researchers working in the field of ecological modeling. Allee, in 1930s, put forward his observation that in many species, the growth and population density are positively correlated. Biological phenomena like difficulty in mating and reduced anti-predator defense lead to the Allee effect. Numerous predator–prey systems have been studied considering strong Allee effect [3, 15, 55, 56, 62, 63] for its ecological significance. Along with the modified growth term, predator functional response plays a key role in modulating predator–prey dynamics. Predation usually involves searching of food entity and food sharing. Ratio-dependent functional response, that stands on the ratio of prey and predator population instead of depending on only prey population, better captures the mutual interference among predators [13, 19]. Interestingly, for ratio-dependent predator–prey system, both the populations may extinct even in presence of stable co-existence equilibrium in the system. Many researchers studied the predator–prey dynamics considering functional response to be ratio-dependent [15, 16, 21, 23, 53, 60]. Besides the consumptive effect of predator, the growth of prey species is also influenced by the non-consumptive effect. That is, only the presence of predator brings substantial psychological and behavioral changes in prey species [14, 46, 49, 59]. The change in foraging behavior and spending more effort and time in vigilance to counter the fear of predation attributes to reduction in the growth rate of species. A significant number of modeling-based studies have been done to see the impact of fear on the dynamics of different predator–prey system [18, 28, 40–42, 51, 57]. Cong *et al.* [12] and Verma *et al.* [52] studied the role of fear in a three-species food chain model. Panday *et al.* [36] observed that fear induces trophic cascading in a three species food chain model.

An ecosystem is seldom stable, rather it is a very dynamic system and is always in recovering phase. However, sometimes, a particular entity of an ecosystem, i.e. a species becomes badly affected mainly due to over-exploitation and environmental factors. The affected species may even reach at the verge of extinction. In this paper, we provide a theoretical study to avoid the extinction of a species that occupy a

relatively lower trophic level in a food chain. We conceptualize the introduction of apex predator as a species conservation tool.

Specific research questions, we intend to address in this study, are as follows:

- If the density of a species depleted below a certain threshold, i.e. viable population size, which triggers the chance of extinction of the species, then how the extinction can be avoided and density of the species can be restored naturally?
- In modeling phenomena, we incorporate the impact of predation induced fear along with direct killing. How these fear parameters mediate the dynamics of the proposed systems?

2. Mathematical Model

Suppose x is the density of our target species, which takes the place of prey in a predator–prey interaction. y is the density of predator (mesopredator) population, which totally depends on the considered prey species for food. In previous studies, predator functional response, i.e. per capita predator's food consumption per unit time, was thought to be a function of prey density only (Holling type I, II, and III functional responses), which covers a huge volume of literature. However, over the course of time, with ecological justifications, it is believed that predator density also has a role to play in the predator's functional response. Thereafter, ratio-dependent functional response, a particular form of predator density-dependent response, where food consumption by a predator per unit time is a function of ratio of prey density to predator abundance, becomes popular among many researchers. Outcomes of many field and laboratory experiments support the consideration of ratio-dependent functional response [5, 6, 9]. Kuang and Baretta [27] first analyzed global qualitative behavior of a ratio-dependent predator–prey system in a systematic way. Thereafter, Hsu *et al.* [23] contributed with a more detailed study of global qualitative behavior and answered many open questions left unanswered by Kuang and Baretta. Xiao and Ruan [58] also put light on global behavior in the neighborhood of origin of ratio-dependent predator–prey system. They have investigated different kinds of topological structures in the neighborhood of origin. In many terrestrial and aquatic ecosystems, the growth rate of some species is observed to follow Allee dynamics. At smaller species density, i.e. below a certain threshold population level, net population growth becomes negative. Few studies have been carried out by considering ratio-dependent functional response along with the incorporation of Allee effect in the growth rate of species [3, 10, 26, 43]. In particular, Sen *et al.* [43] explicitly incorporated the Allee factor along with logistic growth term of prey in a predator–prey system with ratio-dependent functional response. In this study, they compare the dynamics of ratio-dependent predator–prey model with and without Allee effect. They concluded that chance of persistent oscillation of species density ceases with the consideration of Allee effect in the ratio-dependent predator–prey system. Surprisingly, the study of non-consumptive effect of predator over prey density (effect of predation fear), where prey's growth rate subjected

to strong Allee effect along with ratio-dependent predator's functional response, is overlooked. Here, first we consider a two species system, where we represent the interaction of two species by a classical predator–prey model with the ratio-dependent Michaelis–Menten-type functional response [24, 25]. Furthermore, the non-consumptive impact of predators, namely, the induction of fear, elicits significant behavioral and physiological alterations in prey species. Predation-induced fear not only contributes to diminished reproductive output [59], but also affects foraging behavior and adult survival [4, 11, 47]. Consequently, the fear of predation influences the inherent reproductive capacity of prey populations. Thus, the reproductive rate is modulated by a declining function of predator abundance and the intensity of predation-induced fear [35, 50, 61]. Let $h(k_1, y)$ represent this decreasing function, where k_1 denotes the intensity of fear and y signifies predator abundance. The biologically pertinent assumptions underlying the formulation of such a function are elucidated as follows:

$$h(0,y)=1, \quad h(k_1,0)=1, \quad \lim_{k_1\to\infty} h(k_1,y)=0,$$
$$\lim_{y\to\infty} h(k_1,y)=0, \quad \frac{\partial h(k_1,y)}{\partial k_1}<0, \quad \frac{\partial h(k_1,y)}{\partial y}<0.$$

The simplest function with these properties is $h(k_1, y) = \frac{1}{1+k_1 y}$, which is also considered by Wang *et al.* [57] and many authors [12, 28, 33, 34] to include the impact of predation induced fear in the growth of prey species. With the incorporation of fear factor and Allee effect in the growth equations of prey, the predator–prey system takes the following form:

$$\begin{cases} \dfrac{dx}{dt} = \dfrac{1}{1+k_1 y} rx\left(1-\dfrac{x}{K}\right)(x-A) - \dfrac{\alpha_1 xy}{x+y}, \\ \dfrac{dy}{dt} = \dfrac{\theta_1 \alpha_1 xy}{x+y} - \delta_1 y, \end{cases} \tag{2.1}$$

where $x(0) > 0$ and $y(0) > 0$. As growth equations of both prey and predator are undefined at $(x, y) = (0, 0)$, we redefine growth rates $\frac{dx}{dt} = 0$, $\frac{dy}{dt} = 0$, at $(x, y) = (0, 0)$. Such modification was first proposed by Xiao and Ruan [58], and thereafter considered in many studies.

It can be easily shown that for $0 < x(0) < A$, $\lim_{t\to\infty} x(t) = 0$, which in turn implies $y(t) \to 0$ as $t \to \infty$. Therefore, for our proposed model system, we consider $x(0) > A$. To understand the relationship between population size of a species and its chances of extinction, ecologists came up with the idea of viable population size [22, 45]. It is the minimum population size range at which preservation method can be successfully accomplished. Prior to applying any conservation strategy on any species, it is very important to predict its viable population size. Let x_c be that critical limit of population size, below which the species is in danger of extinction. This critical value varies from species to species and also depends on various factors such as nature of ecosystem, habitat and environmental factors.

When the population of x-species is large enough, i.e. $x > x_c$, where x_c is an arbitrary chosen threshold population size of x-species, the dynamics is governed by system (2.1). If the population size of x-species depletes and enters into the interval $A < x \leq x_c$, where A is the Allee threshold, then to protect the x-species from further diminution, we consider that top predator species that feeds upon y-species (mesopredator) only but not on x-species, is being introduced in the habitat. With the introduction of top predator, the dynamics of 3-species system is assumed to be governed by the following system of differential equations:

$$\begin{cases} \dfrac{dx}{dt} = \dfrac{1}{1+k_1 y} rx\left(1-\dfrac{x}{K}\right)(x-A) - \dfrac{1}{1+k_2 z}\dfrac{\alpha_1 xy}{x+y}, \\ \dfrac{dy}{dt} = \dfrac{1}{1+k_2 z}\dfrac{\theta_1\alpha_1 xy}{x+y} - \delta_1 y - \alpha_2 yz, \\ \dfrac{dz}{dt} = \theta_2\alpha_2 yz - \delta_2 z^2. \end{cases} \tag{2.2}$$

Initial conditions are $x(0) > 0, y(0) > 0$, and $z(0) > 0$. Again, the growth equations are defined to be $\frac{dx}{dt} = 0$, $\frac{dy}{dt} = 0$, and $\frac{dz}{dt} = 0$, at $(x, y, z) = (0, 0, 0)$. Here, along with the impact of direct predation of top predator, the non-consumptive effect is also taken into account in governing the dynamics of mesopredator and hence prey species. In addition to impeding growth, fear also impacts the effective predation by mesopredators. A field investigation by Gordon *et al.* [17] furnished compelling evidence of the suppression of foraging and predatory behavior among mesopredators (e.g. feral cats) in the presence of apex predators (e.g. dingoes), thereby mitigating the perceived predation risk encountered by small prey, such as desert rodents. Moreover, within the Yellowstone National Park ecosystem, the reintroduction of apex predators like wolves has brought about substantial shifts in the behavior and grazing patterns of elk [39]. Consequently, in our proposed model, both the growth and predation terms concerning mesopredators are subject to multiplication by a factor of $(1/1 + k_2 z)$, representing a diminishing function of the fear parameter (k_2) and the density of top predators (z). Description of all the parameters that appeared in system (2.2) is mentioned in Table 1. It is to be noted that, we define x-species as prey, y-species as mesopredator and z-species as top predator, throughout the paper. We intend to study the effect of introduction of top predator on the density of our targeted prey species and explore the whole dynamics exhibited by systems (2.1) and (2.2).

Now, we show that solution of system (2.1) satisfies the positivity and boundedness criteria. From system (2.1), we have

$$x(t) = x(0)\exp\left[\int_0^t \left(\frac{r}{1+k_1 y(u)}\left(1-\frac{x(u)}{K}\right)(x(u)-A) - \frac{\alpha_1 y(u)}{x(u)+y(u)}\right)du\right],$$

$$y(t) = y(0)\exp\left[\int_0^t \left(\frac{\theta_1\alpha_1 x(u)}{x(u)+y(u)} - \delta_1\right)du\right].$$

Table 1. Parameters and their description.

Parameter	Description
r	Per capita growth rate of prey
K	Carrying capacity of prey
A	Allee threshold
k_1	Strength of predation fear among prey species
α_1	Predation rate of mesopredator
θ_1	Conversion efficiency of mesopredator
δ_1	Natural death rate of mesopredator
k_2	Strength of predation fear among mesopredator
α_2	Predation rate of top predator
θ_2	Conversion efficiency of top predator
δ_2	Density-dependent death rate of top predator

Therefore, $x(0) > 0$ and $y(0) > 0$ imply $x(t) \geq 0,\ \ y(t) \geq 0,\ \forall\ t \geq 0$. Hence, the solution trajectories initiated from positive quadrant of $x - y$ plane stay in the positive quadrant.

To show boundedness of the system, consider

$$x(t) = x(0) \exp\left[\int_0^t F(x(u), y(u))du\right],$$

where

$$F(x(u), y(u)) = \frac{r}{1 + k_1 y(u)}\left(1 - \frac{x(u)}{K}\right)(x(u) - A) - \frac{\alpha_1 y(u)}{x(u) + y(u)}.$$

Now, we discuss two cases.

Case I. $x(0) \in (0, K)$.

We intend to show $x(t) \leq K,\ \forall\ t \geq 0$. On the contrary, suppose there exist two positive values of t; T_1 and T_2 such that $x(T_1) = K$ and $x(t) > K,\ \forall\ t \in (T_1, T_2)$. Then for all $t \in (T_1, T_2)$,

$$\begin{aligned} x(t) &= x(0) \exp\left[\int_0^t F(x(u), y(u))du\right] \\ &= x(0) \exp\left[\int_0^{T_1} F(x(u), y(u))du\right] \exp\left[\int_{T_1}^t F(x(u), y(u))du\right] \\ &= x(T_1) \exp\left[\int_{T_1}^t F(x(u), y(u))du\right] \\ &< x(T_1) = K, \end{aligned}$$

which is contradictory to our assumption. Therefore, $x(t) \leq K$ for all $t > 0$.

Case II. $x(0) > K$.

As $F(x(t), y(t)) \leq 0$ for $x(t) \geq K$, therefore whenever $x(t) \geq K$,

$$x(t) = x(0) \exp\left[\int_0^t F(x(u), y(u))du\right] \leq x(0).$$

Combining two cases, we get

$$x(t) \leq \max\{K, x(0)\}.$$

Again, system (2.1) implies

$$\frac{dx(t)}{dt} + \frac{1}{\theta_1}\frac{dy(t)}{dt} \leq rx\left(1 - \frac{x}{K}\right)(x - A) - \frac{\delta_1 y}{\theta_1}.$$

Letting $\gamma = \max_{t\geq 0}\{rx(1 - \frac{x}{K})(x - A) + \delta_1 x\}$,

$$\frac{d}{dt}\left(x(t) + \frac{1}{\theta_1}y(t)\right) \leq \gamma - \delta_1\left(x(t) + \frac{1}{\theta_1}y(t)\right).$$

Using Gronwall's inequality, we have

$$\left(x(t) + \frac{1}{\theta_1}y(t)\right) \leq \left(x(0) + \frac{1}{\theta_1}y(0)\right)e^{-\delta_1 t} + \frac{\gamma}{\delta_1}(1 - e^{-\delta_1 t}).$$

As $\delta_1 > 0$, so for sufficiently large time, we get the inequality

$$\left(x(t) + \frac{1}{\theta_1}y(t)\right) \leq \frac{\gamma}{\delta_1} + \epsilon,$$

ϵ takes any positive value. Therefore, $y(t)$ is also bounded.

In a similar manner, for system (2.2), we can have

$$x(t) \leq \max\{x(0), K\}$$

and

$$\begin{aligned}\frac{dx(t)}{dt} + \frac{1}{\theta_1}\frac{dy(t)}{dt} &\leq rx\left(1 - \frac{x}{K}\right)(x - A) - \frac{\delta_1 y}{\theta_1} - \frac{\alpha_2 yz}{\theta_1}.\\ &\leq rx\left(1 - \frac{x}{K}\right)(x - A) - \frac{\delta_1 y}{\theta_1}\\ &\leq \gamma - \delta_1\left(x(t) + \frac{1}{\theta_1}y(t)\right).\end{aligned}$$

Therefore, with similar argument as above, $x(t)$ and $y(t)$ are bounded as for large time, $(x(t) + \frac{1}{\theta_1}y(t)) \leq \frac{\gamma}{\delta_1} + \epsilon$, ϵ takes any positive value. Now, $\frac{dz}{dt} \leq \theta_2\alpha_2 y_{\max} z - \delta_2 z^2$ implies $z(t) \leq \max\{z(0), \frac{\theta_2\alpha_2 y_{\max}}{\delta_2}\}$, $y_{\max}$ is the upper bound of y.

3. Dynamics of the System (2.1)

3.1. *Equilibria of system* (2.1) *and their stability*

Along with trivial equilibrium $E_0(0,0)$, the predator-free equilibria $E_1(A,0)$ and $E_2(K,0)$ are always feasible. Solution of the following two algebraic equations gives feasible coexistence equilibrium $E^*(x^*,y^*)$:

$$\frac{r}{1+k_1y}\left(1-\frac{x}{K}\right)(x-A)-\frac{\alpha_1 y}{x+y}=0,$$

$$\frac{\theta_1\alpha_1 x}{x+y}-\delta_1=0.$$

From the second equation, we have

$$y=\frac{\theta_1\alpha_1-\delta_1}{\delta_1}x. \tag{3.1}$$

Using this value of y in first equation, we get

$$r\left(1-\frac{x}{K}\right)(x-A)=\frac{\theta_1\alpha_1-\delta_1}{\theta_1}\left(1+k_1\frac{\theta_1\alpha_1-\delta_1}{\delta_1}x\right). \tag{3.2}$$

Simplifying, we get

$$x^2+a_1x+a_2=0, \tag{3.3}$$

where

$$a_1=\frac{Kk_1(\theta_1\alpha_1-\delta_1)^2}{r\theta_1\delta_1}-(K+A) \quad \text{and} \quad a_2=\frac{K}{r}\left(rA+\frac{\theta_1\alpha_1-\delta_1}{\theta_1}\right).$$

Therefore, system (2.1) has two co-existence equilibria if $\theta_1\alpha_1-\delta_1>0, a_1<0$ and $a_1^2>4a_2$. These two equilibria collide when $a_1^2=4a_2$ and vanish for $a_1^2<4a_2$. These conditions raise the possibility for system (2.1) to exhibit saddle-node bifurcation, provided $\theta_1\alpha_1-\delta_1>0$ and $a_1<0$ hold.

Trivial equilibrium $E_0(0,0)$ is non-hyperbolic attractor for all parameter values, which can be proved as per [15, Lemma 3]. The equilibrium $E_1(A,0)$ is always unstable, whereas the stability of equilibrium $E_2(K,0)$ depends on the sign of $\theta_1\alpha_1-\delta_1$. Equilibrium E_2 is stable only when the maximum per capita growth rate of mesopredator is negative, i.e. $\theta_1\alpha_1-\delta_1<0$. In that case, only prey population survive and mesopredator population extinct. E_2 becomes unstable when the sign of $\theta_1\alpha_1-\delta_1$ changes to positive. Thus, system (2.1) shows transcritical bifurcation between $E_2(K,0)$ and coexistence equilibrium, provided co-existence equilibrium exist. The Jacobian matrix at $E^*(x^*,y^*)$ is

$$J_{E^*}=\begin{bmatrix} \dfrac{h'(x^*)}{1+k_1y^*}-\dfrac{(\theta_1\alpha_1-\delta_1)^2}{\theta_1^2\alpha_1} & -\dfrac{k_1}{1+k_1y^*}\dfrac{\delta_1y^*}{\theta_1}-\dfrac{\delta_1^2}{\theta_1^2\alpha_1} \\ \dfrac{(\theta_1\alpha_1-\delta_1)^2}{\theta_1\alpha_1} & -\dfrac{\delta_1}{\theta_1\alpha_1}(\theta_1\alpha_1-\delta_1) \end{bmatrix}, \tag{3.4}$$

where $h(x) = xf(x) = rx\left(1 - \frac{x}{K}\right)(x - A)$. Now, we define

$$\Lambda = \text{Trace}(J_{E^*}) = \frac{h'(x^*)}{1 + k_1 y^*} - \frac{(\theta_1\alpha_1 - \delta_1)^2}{\theta_1^2\alpha_1} - \frac{\delta_1}{\theta_1\alpha_1}(\theta_1\alpha_1 - \delta_1), \quad \text{and}$$

$$\Delta = \text{Det}(J_{E^*}).$$

Some calculation results that $\Delta = \text{Det}(J_{E^*}) < (\text{or} >)0$ if $\frac{h'(x^*)}{1+2k_1y^*} > (\text{or} <)\frac{\theta_1\alpha_1 - \delta_1}{\theta_1}$.

Therefore, we can conclude that E^* is locally stable only when

$$h'(x^*) < \min\left[(1 + 2k_1y^*)\left(\frac{\theta_1\alpha_1 - \delta_1}{\theta_1}\right),\right.$$
$$\left.(1 + k_1y^*)\left(\frac{(\theta_1\alpha_1 - \delta_1)^2}{\theta_1^2\alpha_1} + \frac{\delta_1}{\theta_1\alpha_1}(\theta_1\alpha_1 - \delta_1)\right)\right].$$

Also, it is very clear that if $h'(x^*)$ is negative, then the equilibrium E^* is always stable.

Remark 1. From Eq. (3.3), it is to be noted that the x-component of the stable co-existence equilibrium is $x = \frac{-a_1 + \sqrt{a_1^2 - 4a_2}}{2}$, where $a_1 < 0$ and $a_1^2 - 4a_2 > 0$. Now, $\frac{dx}{dk_1} = \frac{1}{2}\frac{da_1}{dk_1}\frac{1}{\sqrt{a_1^2-4a_2}}\{a_1 - \sqrt{a_1^2 - 4a_2}\} < 0$, since $\frac{da_1}{dk_1} = \frac{K(\theta_1\alpha_1-\delta_1)^2}{r\theta_1\delta_1} > 0$. Also, $\frac{dx}{d\alpha_1} = \frac{1}{2}\frac{da_1}{d\alpha_1}\frac{1}{\sqrt{a_1^2-4a_2}}\{a_1 - \sqrt{a_1^2 - 4a_2}\} - \frac{2}{\sqrt{a_1^2-4a_2}}\frac{da_2}{d\alpha_1} < 0$, as $\frac{da_1}{d\alpha_1} = \frac{2Kk_1(\theta_1\alpha_1-\delta_1)}{r\delta_1} > 0$ and $\frac{da_2}{d\alpha_1} = \frac{K}{r} > 0$.

Therefore, it is evident that equilibrium density of prey species always follow decreasing trend with increasing k_1 and α_1, whenever the equilibrium is feasible.

3.2. *Bifurcation analysis of system* (2.1)

Here, first we show the occurrence of transcritical bifurcation by using *Sotomayor theorem* [37]. As $E_2(K, 0)$ changes its stability at $\theta_1\alpha_1 - \delta_1 = 0$. Therefore, we will look for transcritical bifurcation around $E_2(K, 0)$ with respect to the parameter α_1. At E_2, the Jacobian matrix of model system (2.1) is

$$J_{E_2} = \begin{bmatrix} -r(K - A) & -\alpha_1 \\ 0 & (\theta_1\alpha_1 - \delta_1) \end{bmatrix}. \tag{3.5}$$

At $\alpha_1 (= \alpha_1^*) = \frac{\delta_1}{\theta_1}$, the matrix J_{E_2} has simple zero eigenvalue. The eigenvectors of J_{E_2} and $J_{E_2}^T$ corresponding to zero eigenvalue are $V = (v_1, v_2)^T = (\frac{-\alpha_1}{r(K-A)}, 1)^T$ and $W = (w_1, w_2)^T = (0, 1)^T$, respectively.

Consider, $G = (g^1, g^2)^T$, where

$$g^1 = \frac{r}{1 + k_1 y}x\left(1 - \frac{x}{K}\right)(x - A) - \frac{\alpha_1 xy}{x + y},$$

$$g^2 = \frac{\theta_1\alpha_1 xy}{x + y} - \delta_1 y.$$

Now,

$$W^T G_{\alpha_1}(E_2, \alpha_1^*) = w_2 \frac{\partial g^2}{\partial \alpha}\bigg|_{(E_2,\alpha_1^*)} = 0.$$

$$W^T [DG_{\alpha_1}(E_2, \alpha_1^*)V] = w_2 v_2 \frac{\partial^2 g^2}{\partial \alpha_1 \partial y}\bigg|_{(E_2,\alpha_1^*)} = \theta_1 \neq 0.$$

$$W^T [D^2 G(E_2, \alpha_1^*)(V, V)] = w_2 v_2^2 \frac{\partial^2 g^2}{\partial y^2}\bigg|_{(E_2,\alpha_1^*)} = -\frac{2\delta_1}{K} \neq 0.$$

Therefore, according to *Sotomayor theorem* [37], the conditions for the existence of transcritical bifurcation are satisfied. Hence, transcritical bifurcation occurs at $\alpha_1 = \alpha_1^*$ for system (2.1), that is as α_1 crosses α_1^*, the equilibrium E_2 changes its stability and emergence (or vanishing) of a stable interior equilibrium is observed.

As mentioned in Remark 1, two co-existence equilibria collide and vanish at $(\tilde{x}, \tilde{y})$, where $f'(\tilde{x}) = k_1 \frac{(\theta_1\alpha_1 - \delta_1)^2}{\theta_1 \delta_1}$. Corresponding $\tilde{x}$ and $\tilde{y}$ are given by $\tilde{x} = \frac{1}{2}\left[(K + A) - K k_1 \frac{(\theta_1\alpha_1 - \delta_1)^2}{r\theta_1\delta_1}\right]$ and $\tilde{y} = \frac{\theta_1\alpha_1}{\delta_1}\tilde{x}$. As two equilibrium collide at $(\tilde{x}, \tilde{y})$, discriminant of Eq. (3.3) becomes zero, which gives a critical value of k_1, $\tilde{k}_1$ say. Now, we check the conditions of *Sotomayor theorem* [37] for saddle-node bifurcation.

Let the eigenvectors corresponding to zero eigenvalue be $\bar{V} = (\bar{v}_1, \bar{v}_2)^T$ and $\bar{W} = (\bar{w}_1, \bar{w}_2)^T$ for $J_{\tilde{E}}$ and $J_{\tilde{E}}^T$, respectively. Then

$$\bar{V} = \begin{pmatrix} 1 \\ \dfrac{\theta_1\alpha_1 - \delta_1}{\delta_1} \end{pmatrix}, \quad \text{and} \quad \bar{W} = \begin{pmatrix} 1 \\ \dfrac{-\frac{k_1}{1+k_1\tilde{y}}\frac{\delta_1}{\theta_1}\tilde{y} + \frac{\delta_1^2}{\theta_1^2\alpha_1}}{\delta_1(\frac{\theta_1\alpha_1 - \delta_1}{\theta_1\alpha_1})} \end{pmatrix}.$$

Considering

$$G(x, y, k_1) = \begin{pmatrix} \dfrac{1}{1 + k_1 y} x f(x) - \dfrac{\alpha_1 x y}{x + y} \\ \dfrac{\theta_1 \alpha_1 x y}{x + y} - \delta_1 y \end{pmatrix},$$

we obtain

$$\bar{W}^T G_{k_1}(\tilde{x}, \tilde{y}, \tilde{k}_1) = -\frac{\tilde{y}}{(1 + \tilde{k}_1\tilde{y})^2} r\tilde{x}\left(1 - \frac{\tilde{x}}{K}\right)(\tilde{x} - A) < 0$$

and

$$\bar{W}^T [D^2 G(\tilde{x}, \tilde{y}, \tilde{k}_1)(\bar{V}, \bar{V})] = -\frac{2r}{K}\frac{\tilde{x}}{1 + \tilde{k}_1\tilde{y}} < 0.$$

Hence, by *Sotomayor theorem*, we affirm that system (2.1) undergoes saddle-node bifurcation around $\tilde{E} = (\tilde{x}, \tilde{y})$ as k_1 crosses a critical value $\tilde{k}_1$.

Occurrence or termination of limit cycle with varying parameter is characterized by Hopf bifurcation. Choosing strength of fear k_1 as the bifurcation parameter, we

intend to show analytically that system (2.1) exhibits Hopf bifurcation at interior equilibrium $E^*(x^*, y^*)$. Conditions for occurrence of Hopf bifurcation for system (2.1) are mentioned in the following theorem.

Theorem 3.1. *System* (2.1) *undergoes Hopf bifurcation around the co-existence equilibrium* $E^*(x^*, y^*)$ *at* $k_1 = k_1^*$ *if and only if* $\frac{h'(x^*)}{1+2k_1y^*} < \frac{\theta_1\alpha_1-\delta_1}{\theta_1}$ *and* $\frac{d}{dk_1}(\Lambda)|_{k_1=k_1^*} \neq 0$, *where* $\Lambda = \text{Trace}(J_{E^*})$.

Proof. At Hopf bifurcation point, the pair of eigenvalues of the Jacobian matrix at E^* should be purely imaginary. Therefore, the Jacobian matrix (3.4) has trace Λ equal to zero for the critical value $k_1 = k_1^*$, which leads the corresponding characteristic equation to become

$$\lambda^2 + \Delta_{k_1=k_1^*} = 0.$$

Let the pair of purely imaginary roots of the above equation be $\lambda_{1,2} = \pm\iota\phi_0$, where $\phi_0 = \sqrt{\Delta}_{k_1=k_1^*}$ exists, if $\Delta > 0$. Therefore, at $k_1 = k_1^*$

$$\frac{h'(x^*)}{1+2k_1y^*} < \frac{\theta_1\alpha_1-\delta_1}{\theta_1}.$$

Suppose the eigenvalues of the Jacobian matrix for any neighboring point k_1 of k_1^* are $\lambda_{1,2} = \xi(k_1) \pm \iota\phi(k_1)$, where

$$\xi(k_1) = \frac{\Lambda(x^*(k_1), y^*(k_1))}{2}, \quad \phi(k_1) = \sqrt{\Delta(x^*(k_1), y^*(k_1)) - \frac{\Lambda^2(x^*(k_1), y^*(k_1))}{4}}.$$

Now,

$$\frac{d}{dk_1}\xi(k_1)|_{k_1=k_1^*} = \frac{1}{2}\left[\frac{d}{dk_1}\Lambda(x^*(k_1), y^*(k_1))\right]_{k_1=k_1^*}.$$

Transversality condition affirms the crossing of imaginary axis for the eigenvalues with nonzero speed. The transversality condition is satisfied if $\frac{d}{dk_1}\Lambda(x^*(k_1), y^*(k_1)) \neq 0$ at $k_1 = k_1^*$, i.e. if $h''(x^*)\frac{dx^*}{dk_1}|_{k_1=k_1^*} \neq \frac{(\theta_1\alpha_1-\delta_1)^2}{\theta_1^2\alpha_1\delta_1}(\theta_1\alpha_1 - \delta_1 + \theta_1\delta_1)(x^* + k_1\frac{dx^*}{dk_1})|_{k_1=k_1^*}$. Therefore, with these conditions, system (2.1) would undergo Hopf bifurcation at $k_1 = k_1^*$. □

4. Dynamics of System (2.2)

4.1. *Existence of interior equilibria*

Positive solution of following three algebraic equations gives the co-existence equilibrium of system (2.2):

$$\frac{1}{1+k_1y}r\left(1-\frac{x}{K}\right)(x-A) - \frac{1}{1+k_2z}\frac{\alpha_1 y}{x+y} = 0, \tag{4.1}$$

$$\frac{1}{1+k_2z}\frac{\theta_1\alpha_1 x}{x+y} - \delta_1 - \alpha_2 z = 0, \tag{4.2}$$

$$\theta_2\alpha_2 y - \delta_2 z = 0. \tag{4.3}$$

From (4.3), we have

$$z = \frac{\theta_2\alpha_2}{\delta_2} y. \tag{4.4}$$

Using this value of z in Eqs. (4.1) and (4.2), we get

$$r\left(1 - \frac{x}{K}\right)(x - A) = \frac{\alpha_1 y}{x + y} \frac{1 + k_1 y}{1 + k_2 \frac{\theta_2\alpha_2}{\delta_2} y}, \tag{4.5}$$

$$\frac{\theta_1\alpha_1 x}{x + y} = \left(\delta_1 + \alpha_2 \frac{\theta_2\alpha_2}{\delta_2} y\right)\left(1 + k_2 \frac{\theta_2\alpha_2}{\delta_2} y\right). \tag{4.6}$$

The curve (4.6) approaches origin and always increases in the positive quadrant. On the other hand, the curve (4.5) passes through $(A, 0)$ and $(K, 0)$; increasing at $(A, 0)$ and decreasing at $(K, 0)$. Therefore, these two isoclines may have no intersection,

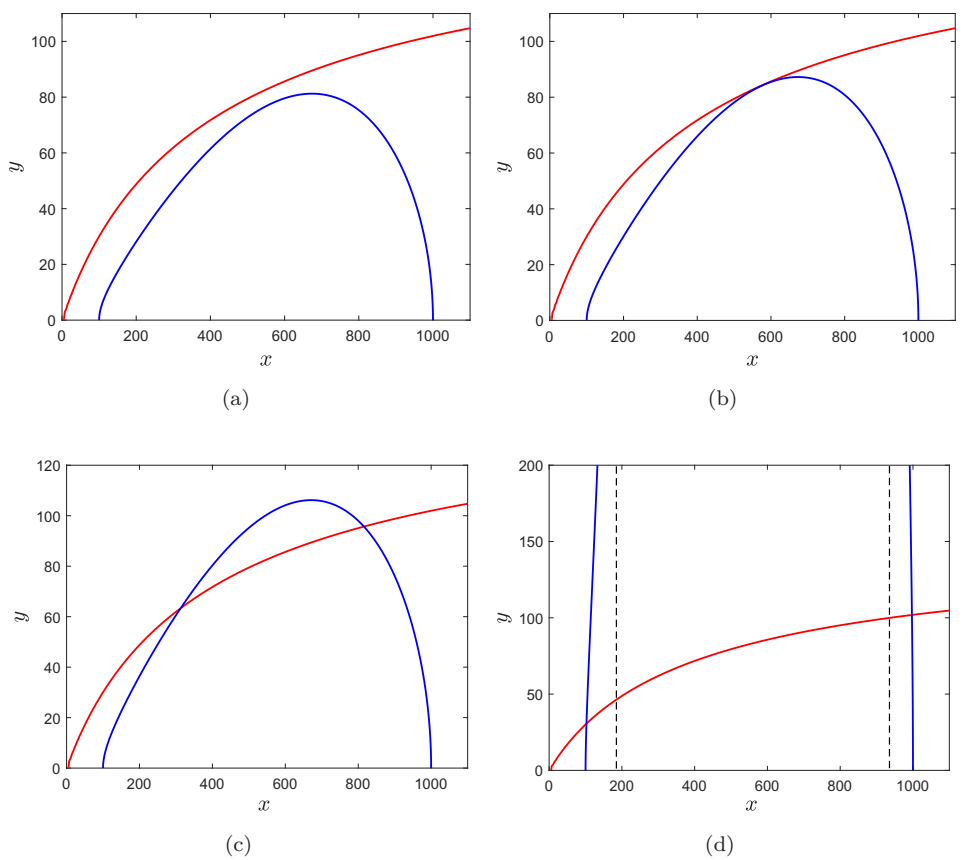

Fig. 1. (Color online) Different scenarios for the intersection of two isoclines. Blue and red curves represent isoclines (4.5) and (4.6), respectively. The value of fear parameter k_1 is varied and its values are (a) $k_1 = 16$, (b) $k_1 = 14.08$, (c) $k_1 = 10$, (d) $k_1 = 0.1$, and other parameter values are same as given in Eq. (5.2).

one touching point, or two intersections, based upon parameter values, as shown in Figs. 1(a)–1(c). Moreover, the curve (4.5) has two vertical asymptotes if $\frac{(K-A)^2}{4K} > \frac{k_1\alpha_1\delta_2}{rk_2\theta_2\alpha_2}$. In such a case, two isoclines obviously intersect at two points, as shown in Fig. 1(d).

4.2. *Stability and bifurcation analysis of system* (2.2)

Now, the Jacobian matrix at co-existence equilibrium $\hat{E} = (\hat{x}, \hat{y}, \hat{z})$ is

$$J_{\hat{E}} = \begin{bmatrix} b_{11} & b_{12} & b_{13} \\ b_{21} & b_{22} & b_{23} \\ b_{31} & b_{32} & b_{33} \end{bmatrix}, \tag{4.7}$$

where

$$b_{11} = \frac{\hat{x}f'(\hat{x}) + f(\hat{x})}{1 + k_1\hat{y}} - \frac{1}{1 + k_2\hat{z}}\frac{\alpha_1\hat{y}^2}{(\hat{x} + \hat{y})^2}, \quad b_{21} = \frac{1}{1 + k_2\hat{z}}\frac{\theta_1\alpha_1\hat{y}^2}{(\hat{x} + \hat{y})^2}, \quad b_{31} = 0,$$

$$b_{12} = -\frac{\hat{x}f(\hat{x})k_1}{(1 + k_1\hat{y})^2} - \frac{1}{1 + k_2\hat{z}}\frac{\alpha_1\hat{x}^2}{(\hat{x} + \hat{y})^2}, \quad b_{22} = -\frac{\hat{y}}{\hat{x} + \hat{y}}(\delta_1 + \alpha_2\hat{z}), \quad b_{32} = \theta_2\alpha_2\hat{z},$$

$$b_{13} = \frac{k_2}{(1 + k_2\hat{z})^2}\frac{\alpha_1\hat{x}\hat{y}}{(\hat{x} + \hat{y})}, \quad b_{23} = -\frac{k_2}{(1 + k_2\hat{z})^2}\frac{\theta_1\alpha_1\hat{x}\hat{y}}{(\hat{x} + \hat{y})} - \alpha_2\hat{y}, \quad b_{33} = -\delta_2\hat{y}.$$

The characteristic equation corresponding to the Jacobian matrix is

$$\mu^3 + B_1\mu^2 + B_2\mu + B_3 = 0 \tag{4.8}$$

where

$$B_1 = -(b_{11} + b_{22} + b_{33}),$$

$$B_2 = b_{11}b_{22} + b_{11}b_{33} + b_{22}b_{33} - b_{12}b_{21} - b_{23}b_{32},$$

$$B_3 = b_{12}b_{21}b_{33} - b_{11}b_{22}b_{33} - b_{13}b_{21}b_{32} + b_{11}b_{23}b_{32}.$$

According to the Routh–Hurwitz criterion, the roots of Eq. (4.8) lie on the left half of a complex plane if and only if $B_1 > 0,\ B_3 > 0,$ and $B_1B_2 - B_3 > 0$. Therefore, with these conditions, the equilibrium $\hat{E} = (\hat{x}, \hat{y}, \hat{z})$ is locally asymptotically stable.

4.3. *Hopf bifurcation*

Suppose at some critical value of α_2 (α_2^* *say*), the conditions $B_1 > 0$ and $B_3 > 0$ hold but $B_1B_2 - B_3 = 0$. Then, the characteristic equation (4.8) can be written as

$$(\mu^2 + B_2)(\mu + B_1) = 0. \tag{4.9}$$

The above equation has two purely imaginary roots, say $\mu_{1,2} = \pm\iota\sqrt{B_2}$ and a negative real root, say $\mu_3 = -B_1$.

Now, suppose at any point α_2 in the ϵ-neighborhood of α_2^*, $\mu_{1,2} = \gamma_1 \pm \iota\gamma_2$. Putting this in the characteristic equation and separating real and imaginary parts, we get

$$\gamma_1^3 - 3\gamma_1\gamma_2^2 + B_1\gamma_1^2 - B_1\gamma_2^2 + B_2\gamma_1 + B_3 = 0, \tag{4.10}$$

$$3\gamma_1^2\gamma_2 - \gamma_2^3 + 2B_1\gamma_1\gamma_2 + B_2\gamma_2 = 0. \tag{4.11}$$

As $\gamma_2 \neq 0$, from Eq. (4.11), we have

$$\gamma_2^2 = 3\gamma_1^2 + 2B_1\gamma_1 + B_2.$$

Using this value of γ_2 in Eq. (4.10), we get

$$8\gamma_1^3 + 8B_1\gamma_1^2 + 2\gamma_1(B_1^2 + B_2) + B_1B_2 - B_3 = 0.$$

Differentiating above equation with respect to α_2 and using the fact that $\gamma_1(\alpha_2^*) = 0$, we get

$$\left[\frac{d\gamma_1}{d\alpha_2}\right]_{\alpha_2=\alpha_2^*} = -\left[\frac{1}{2(B_1^2 + B_2)}\frac{d}{d\alpha_2}(B_1B_2 - B_3)\right]_{\alpha_2=\alpha_2^*}.$$

Hence, transversality condition holds if $\frac{d}{d\alpha_2}(B_1B_2 - B_3)|_{\alpha_2=\alpha_2^*} \neq 0$. Therefore, with this condition, system (2.2) exhibits Hopf bifurcation at $\alpha_2 = \alpha_2^*$ around interior equilibrium $\hat{E}$. System (2.2) also shows saddle-node bifurcation, which can be proved following the same analysis carried out in Sec. 3.2.

4.4. *Bogdanov–Takens bifurcation*

Bogdanov–Takens bifurcation (BT-bifurcation) is a type of codimension-2 bifurcation. At BT-bifurcation point, the system has zero eigenvalue with multiplicity 2. Using the methods from Kuznetsov [29], we derive the conditions for BT-bifurcation at $\hat{E}$ of the model system (2.2).

To examine the conditions for BT-bifurcation of system (2.2) at $\hat{E}$, first we use the transformations $x = \hat{x} + \bar{X}$, $y = \hat{y} + \bar{Y}$, and $z = \hat{z} + \bar{Z}$ in order to shift the origin at $\hat{E} = (\hat{x}, \hat{y}, \hat{z})$. Consequently, system (2.2) can be expressed in the subsequent form:

$$\begin{bmatrix} \bar{X} \\ \bar{Y} \\ \bar{Z} \end{bmatrix}' = J_{\hat{E}} \begin{bmatrix} \bar{X} \\ \bar{Y} \\ \bar{Z} \end{bmatrix} + \begin{bmatrix} \hat{C}_1 \\ \hat{C}_2 \\ \hat{C}_3 \end{bmatrix} + \mathcal{O}(|\bar{X}, \bar{Y}, \bar{Z}|^3), \tag{4.12}$$

where

$$\hat{C}_1 = l^1_{200}\bar{X}^2 + l^1_{020}\bar{Y}^2 + l^1_{002}\bar{Z}^2 + l^1_{110}\bar{X}\bar{Y} + l^1_{101}\bar{X}\bar{Z} + l^1_{011}\bar{Y}\bar{Z},$$

$$\hat{C}_2 = l^2_{200}\bar{X}^2 + l^2_{020}\bar{Y}^2 + l^2_{002}\bar{Z}^2 + l^2_{110}\bar{X}\bar{Y} + l^2_{101}\bar{X}\bar{Z} + l^2_{011}\bar{Y}\bar{Z},$$

$$\hat{C}_3 = -\delta_2\bar{Z}^2 + \theta_2\alpha_2\bar{Y}\bar{Z}$$

and

$$l^1_{200} = -\frac{r(2\hat{x}-A)}{K(1+k_1\hat{y})} + \frac{r(1-\frac{\hat{x}}{A})}{K(1+k_1\hat{y})}\frac{\alpha_1\hat{y}^2}{(\hat{x}+\hat{y})^3(1+k_2\hat{z})},$$

$$l^1_{110} = -\frac{r\hat{x}k_1(1-\frac{\hat{x}}{K})}{K(1+k_1\hat{y})} + \frac{2r\hat{x}k_1 - rKk_1}{K(1+k_1\hat{y})^2}(\hat{x}-A) - \frac{2\alpha_1\hat{x}\hat{y}}{(\hat{x}+\hat{y})^3(1+k_2\hat{z})},$$

$$l^1_{020} = \frac{\alpha_1\hat{x}^2}{(\hat{x}+\hat{y})^3(1+k_2\hat{z})} + \frac{r\hat{x}k_1(1-\frac{\hat{x}}{K})(\hat{x}-A)}{(1+k_1\hat{y})^3},$$

$$l^1_{002} = -\frac{\alpha_1k_2^2\hat{x}\hat{y}}{(\hat{x}+\hat{y})(1+k_2\hat{z})^3}, \quad l^1_{101} = \frac{\alpha_1k_2\hat{y}^2}{(\hat{x}+\hat{y})^2(1+k_2\hat{z})^2},$$

$$l^1_{011} = \frac{\alpha_1k_2\hat{x}^2}{(\hat{x}+\hat{y})^2(1+k_2\hat{z})^2}, \quad l^2_{200} = -\frac{\theta_1\alpha_1\hat{y}^2}{(\hat{x}+\hat{y})^3(1+k_2\hat{z})},$$

$$l^2_{020} = -\frac{\theta_1\alpha_1\hat{x}^2}{(\hat{x}+\hat{y})^3(1+k_2\hat{z})}, \quad l^2_{002} = \frac{\theta_1\alpha_1k_2^2\hat{x}\hat{y}}{(\hat{x}+\hat{y})(1+k_2\hat{z})^3},$$

$$l^2_{110} = \frac{2\theta_1\alpha_1\hat{x}\hat{y}}{(\hat{x}+\hat{y})^3(1+k_2\hat{z})}, \quad l^2_{101} = -\frac{\theta_1\alpha_1k_2(1+k_2\hat{z})\hat{y}^2}{(\hat{x}+\hat{y})^2(1+k_2\hat{z})^3},$$

$$l^2_{011} = -\frac{\theta_1\alpha_1k_2\hat{x}^2(1+k_2\hat{z})}{(\hat{x}+\hat{y})^2(1+k_2\hat{z})^3} - \alpha_2.$$

The generalized characteristic vectors corresponding to characteristic value $\mu_{1,2} = 0$ are $\tilde{U}_1 = [\tilde{u}_{11}\ \tilde{u}_{21}\ \tilde{u}_{31}]^T$, and $\tilde{U}_2 = [\tilde{u}_{12}\ \tilde{u}_{22}\ \tilde{u}_{32}]^T$ where

$$\tilde{u}_{11} = \frac{b_{22}b_{33} - b_{23}b_{32}}{b_{32}b_{21}}, \quad \tilde{u}_{21} = -\frac{b_{33}}{b_{32}}, \quad \tilde{u}_{31} = 1, \quad \tilde{u}_{12} = \frac{\Delta_1}{\Delta},$$

$$\tilde{u}_{22} = \frac{\Delta_2}{\Delta}, \quad \tilde{u}_{32} = \frac{\Delta_3}{\Delta},$$

where

$$\Delta = \det(J_{\hat{E}}) = \begin{vmatrix} b_{11} & b_{12} & b_{13} \\ b_{21} & b_{22} & b_{23} \\ 0 & b_{32} & b_{33} \end{vmatrix}, \quad \Delta_1 = \begin{vmatrix} \tilde{u}_{11} & b_{12} & b_{13} \\ \tilde{u}_{21} & b_{22} & b_{23} \\ \tilde{u}_{31} & b_{32} & b_{33} \end{vmatrix},$$

$$\Delta_2 = \begin{vmatrix} b_{11} & \tilde{u}_{11} & b_{13} \\ b_{21} & \tilde{u}_{21} & b_{23} \\ 0 & \tilde{u}_{31} & b_{33} \end{vmatrix}, \quad \Delta_3 = \begin{vmatrix} b_{11} & b_{12} & \tilde{u}_{11} \\ b_{21} & b_{22} & \tilde{u}_{21} \\ 0 & b_{32} & \tilde{u}_{31} \end{vmatrix},$$

which satisfy $J_{\hat{E}}\tilde{U}_1 = 0$ and $J_{\hat{E}}\tilde{U}_2 = \tilde{U}_1$. Also, $\tilde{U}_3 = [\tilde{u}_{13}\ \ \tilde{u}_{23}\ \ \tilde{u}_{33}]^T$ is the eigenvector corresponding to characteristic value $\mu_3 = -B_1$, where

$$\tilde{u}_{13} = \frac{(b_{22}+B_1)(b_{33}+B_1) - b_{23}b_{32}}{b_{32}b_{21}}, \quad \tilde{u}_{23} = -\frac{b_{33}+B_1}{b_{32}}, \quad \tilde{u}_{33} = 1.$$

Let $\tilde{\mathcal{P}} = [\tilde{U}_1 \ \ \tilde{U}_2 \ \ \tilde{U}_3]$, then under the non-singular linear transformation

$$\begin{bmatrix} \bar{X} \\ \bar{Y} \\ \bar{Z} \end{bmatrix} = \tilde{\mathcal{P}} \begin{bmatrix} \hat{X}_1 \\ \hat{X}_2 \\ \hat{X}_3 \end{bmatrix},$$

system (4.12) becomes

$$\begin{cases} \hat{X}_1' = \hat{X}_2 + \tilde{A}_{20}\hat{X}_1^2 + \tilde{A}_{11}\hat{X}_1\hat{X}_2 + \tilde{A}_{02}\hat{X}_2^2 + \mathcal{O}(|\hat{X}_1, \hat{X}_2, \hat{X}_3|^2), \\ \hat{X}_2' = \tilde{B}_{20}\hat{X}_1^2 + \tilde{B}_{11}\hat{X}_1\hat{X}_2 + \tilde{B}_{02}\hat{X}_2^2 + \mathcal{O}(|\hat{X}_1, \hat{X}_2, \hat{X}_3|^2), \\ \hat{X}_3' = -B_1\hat{X}_3 + \mathcal{O}(|\hat{X}_1, \hat{X}_2, \hat{X}_3|^2), \end{cases} \tag{4.13}$$

where the inverse of $\tilde{\mathcal{P}}$ is given by

$$\tilde{\mathcal{P}}^{-1} = \begin{bmatrix} \tilde{v}_{11} & \tilde{v}_{12} & \tilde{v}_{13} \\ \tilde{v}_{21} & \tilde{v}_{22} & \tilde{v}_{23} \\ \tilde{v}_{31} & \tilde{v}_{32} & \tilde{v}_{33} \end{bmatrix}.$$

Here,

$$\begin{aligned}
\tilde{A}_{20} &= \tilde{v}_{11}(l^1_{200}\tilde{u}^2_{11} + l^1_{020}\tilde{u}^2_{21} + l^1_{002}\tilde{u}^2_{31} + l^1_{110}\tilde{u}_{11}\tilde{u}_{21} + l^1_{101}\tilde{u}_{11}\tilde{u}_{31} + l^1_{011}\tilde{u}_{21}\tilde{u}_{31}) \\
&\quad + \tilde{v}_{12}(l^2_{200}\tilde{u}^2_{11} + l^2_{020}\tilde{u}^2_{21} + l^2_{002}\tilde{u}^2_{31} + l^2_{110}\tilde{u}_{11}\tilde{u}_{21} + l^2_{101}\tilde{u}_{11}\tilde{u}_{31} + l^2_{011}\tilde{u}_{21}\tilde{u}_{31}) \\
&\quad + \tilde{v}_{13}(-\delta_2\tilde{u}^2_{31} + \theta_2\alpha_2\tilde{u}_{21}\tilde{u}_{31}), \\
\tilde{A}_{11} &= \tilde{v}_{11}(2l^1_{200}\tilde{u}_{11}\tilde{u}_{12} + 2l^1_{020}\tilde{u}_{21}\tilde{u}_{22} + 2l^1_{002}\tilde{u}_{31}\tilde{u}_{32} + l^1_{110}(\tilde{u}_{11}\tilde{u}_{22} + \tilde{u}_{12}\tilde{u}_{21}) \\
&\quad + 2l^1_{101}(\tilde{u}_{11}\tilde{u}_{32} + \tilde{u}_{12}\tilde{u}_{31}) + 2l^1_{011}(\tilde{u}_{22}\tilde{u}_{31} + \tilde{u}_{21}\tilde{u}_{32})) + \tilde{v}_{12}(2l^2_{200}\tilde{u}_{11}\tilde{u}_{12} \\
&\quad + 2l^2_{020}\tilde{u}_{21}\tilde{u}_{22} + 2l^2_{002}\tilde{u}_{31}\tilde{u}_{32} + l^2_{110}(\tilde{u}_{11}\tilde{u}_{22} + \tilde{u}_{12}\tilde{u}_{21}) + 2l^2_{101}(\tilde{u}_{11}\tilde{u}_{32} \\
&\quad + \tilde{u}_{12}\tilde{u}_{31}) + 2l^2_{011}(\tilde{u}_{22}\tilde{u}_{31} + \tilde{u}_{21}\tilde{u}_{32})) + \tilde{v}_{13}(-2\delta_2\tilde{u}_{31}\tilde{u}_{32} + \theta_2\alpha_2(\tilde{u}_{21}\tilde{u}_{32} \\
&\quad + \tilde{u}_{22}\tilde{u}_{31})), \\
\tilde{A}_{02} &= \tilde{v}_{11}(l^1_{200}\tilde{u}^2_{12} + l^1_{020}\tilde{u}^2_{22} + l^1_{002}\tilde{u}^2_{32} + l^1_{110}\tilde{u}_{12}\tilde{u}_{22} + l^1_{101}\tilde{u}_{12}\tilde{u}_{32} + l^1_{011}\tilde{u}_{22}\tilde{u}_{32}) \\
&\quad + \tilde{v}_{12}(l^2_{200}\tilde{u}^2_{12} + l^2_{020}\tilde{u}^2_{22} + l^2_{002}\tilde{u}^2_{32} + l^2_{110}\tilde{u}_{12}\tilde{u}_{22} + l^2_{101}\tilde{u}_{12}\tilde{u}_{32} + l^2_{011}\tilde{u}_{22}\tilde{u}_{32}) \\
&\quad + \tilde{v}_{13}(-\delta_2\tilde{u}^2_{32} + \theta_2\alpha_2\tilde{u}_{22}\tilde{u}_{32}), \\
\tilde{B}_{20} &= \tilde{v}_{21}(l^1_{200}\tilde{u}^2_{11} + l^1_{020}\tilde{u}^2_{21} + l^1_{002}\tilde{u}^2_{31} + l^1_{110}\tilde{u}_{11}\tilde{u}_{21} + l^1_{101}\tilde{u}_{11}\tilde{u}_{31} + l^1_{011}\tilde{u}_{21}\tilde{u}_{31}) \\
&\quad + \tilde{v}_{22}(l^2_{200}\tilde{u}^2_{11} + l^2_{020}\tilde{u}^2_{21} + l^2_{002}\tilde{u}^2_{31} + l^2_{110}\tilde{u}_{11}\tilde{u}_{21} + l^2_{101}\tilde{u}_{11}\tilde{u}_{31} + l^2_{011}\tilde{u}_{21}\tilde{u}_{31}) \\
&\quad + \tilde{v}_{23}(-\delta_2\tilde{u}^2_{31} + \theta_2\alpha_2\tilde{u}_{21}\tilde{u}_{31}),
\end{aligned}$$

$$\begin{aligned}\tilde{B}_{11} &= \tilde{v}_{21}(2l^1_{200}\tilde{u}_{11}\tilde{u}_{12} + 2l^1_{020}\tilde{u}_{21}\tilde{u}_{22} + 2l^1_{002}\tilde{u}_{31}\tilde{u}_{32} + l^1_{110}(\tilde{u}_{11}\tilde{u}_{22} + \tilde{u}_{12}\tilde{u}_{21})\\ &\quad + 2l^1_{101}(\tilde{u}_{11}\tilde{u}_{32} + \tilde{u}_{12}\tilde{u}_{31}) + 2l^1_{011}(\tilde{u}_{22}\tilde{u}_{31} + \tilde{u}_{21}\tilde{u}_{32})) + \tilde{v}_{22}(2l^2_{200}\tilde{u}_{11}\tilde{u}_1\\ &\quad + 2l^2_{020}\tilde{u}_{21}\tilde{u}_{22} + 2l^2_{002}\tilde{u}_{31}\tilde{u}_{32} + l^2_{110}(\tilde{u}_{11}\tilde{u}_{22} + \tilde{u}_{12}\tilde{u}_{21}) + 2l^2_{101}(\tilde{u}_{11}\tilde{u}_{32}\\ &\quad + \tilde{u}_{12}\tilde{u}_{31}) + 2l^2_{011}(\tilde{u}_{22}\tilde{u}_{31} + \tilde{u}_{21}\tilde{u}_{32})) + \tilde{v}_{23}(-2\delta_2\tilde{u}_{31}\tilde{u}_{32}\\ &\quad + \theta_2\alpha_2(\tilde{u}_{21}\tilde{u}_{32} + \tilde{u}_{22}\tilde{u}_{31})),\\ \tilde{B}_{02} &= \tilde{v}_{21}(l^1_{200}\tilde{u}^2_{12} + l^1_{020}\tilde{u}^2_{22} + l^1_{002}\tilde{u}^2_{32} + l^1_{110}\tilde{u}_{12}\tilde{u}_{22} + l^1_{101}\tilde{u}_{12}\tilde{u}_{32} + l^1_{011}\tilde{u}_{22}\tilde{u}_{32})\\ &\quad + \tilde{v}_{22}(l^2_{200}\tilde{u}^2_{12} + l^2_{020}\tilde{u}^2_{22} + l^2_{002}\tilde{u}^2_{32} + l^2_{110}\tilde{u}_{12}\tilde{u}_{22} + l^2_{101}\tilde{u}_{12}\tilde{u}_{32} + l^2_{011}\tilde{u}_{22}\tilde{u}_{32})\\ &\quad + \tilde{v}_{23}(-\delta_2\tilde{u}^2_{32} + \theta_2\alpha_2\tilde{u}_{22}\tilde{u}_{32}).\end{aligned}$$

Hence, in accordance with the center manifold theorem, center manifold exists for system (2.2), and it can be locally expressed in the following manner:

$$\begin{aligned}\hat{\mathbb{X}}^c =&\{(\hat{X}_1, \hat{X}_2, \hat{X}_3) \in \mathbb{R}^2 \times \mathbb{R} \big|\ \hat{X}_3 = \widetilde{F}_1(\hat{X}_1, \hat{X}_2) \text{ for } |\hat{X}_1| < \epsilon_1 \text{ and } |\hat{X}_2| < \epsilon_2,\\ &\widetilde{F}_1(0,0) = D\widetilde{F}_1(0,0) = 0\},\end{aligned}$$

for and sufficiently small ϵ_1 and ϵ_2. Thus, we have to calculate the center manifold for system (2.2). The system is restricted to the central manifold given as

$$\begin{cases}\hat{X}_1' = \hat{X}_2 + \tilde{A}_{20}\hat{X}_1^2 + \tilde{A}_{11}\hat{X}_1\hat{X}_2 + \tilde{A}_{02}\hat{X}_2^2 + \mathcal{O}(|\hat{X}_1, \hat{X}_2|^2),\\ \hat{X}_2' = \tilde{B}_{20}\hat{X}_1^2 + \tilde{B}_{11}\hat{X}_1\hat{X}_2 + \tilde{B}_{02}\hat{X}_2^2 + \mathcal{O}(|\hat{X}_1, \hat{X}_2|^2).\end{cases} \tag{4.14}$$

Using the transformation

$$\begin{cases}\hat{X}_1 = \widetilde{\mathfrak{U}} + \dfrac{1}{2}(\tilde{A}_{11} + \tilde{B}_{02})\widetilde{\mathfrak{U}}^2 + \tilde{A}_{02}\widetilde{\mathfrak{U}}\widetilde{\mathfrak{V}} + \mathcal{O}(|\widetilde{\mathfrak{U}}, \widetilde{\mathfrak{V}}|^2),\\ \hat{X}_2 = \widetilde{\mathfrak{V}} - \tilde{A}_{20}\widetilde{\mathfrak{U}}^2 + \tilde{B}_{02}\widetilde{\mathfrak{U}}\widetilde{\mathfrak{V}} + \mathcal{O}(|\widetilde{\mathfrak{U}}, \widetilde{\mathfrak{V}}|^2),\end{cases} \tag{4.15}$$

and rewriting system (4.14) in $\hat{X}_1$ and $\hat{X}_2$, we get

$$\begin{cases}\hat{X}_1' = \hat{X}_2,\\ \hat{X}_2' = \widetilde{\mathfrak{B}}_{20}\hat{X}_1^2 + \widetilde{\mathfrak{B}}_{11}\hat{X}_1\hat{X}_2,\end{cases} \tag{4.16}$$

where $\widetilde{\mathfrak{B}}_{20} = \tilde{B}_{20}$ and $\widetilde{\mathfrak{B}}_{11} = \tilde{B}_{11} + 2\tilde{A}_{20}$. The conditions derived for the occurrence of BT-bifurcation are summarized in Theorem 4.1.

Theorem 4.1. *If* $\mathfrak{B}_{20}$ *and* $\mathfrak{B}_{11}$ *are nonzero, then system* (2.2) *displays a co-dimension* 2 *BT-bifurcation at the interior equilibrium* $\hat{E}$.

5. Numerical Simulations

This section deals with numerical simulations to explore the underlying dynamics that systems (2.1) and (2.2) posses, with the help of MATLAB software and MATCONT package. Suppose initially the density of prey is large enough such that it

remains above the threshold value x_c. Then the dynamics is governed by system (2.1) and the parameter values we consider for simulations are as follows:

$$r = 2, \quad K = 1000, \quad A = 100, \quad \alpha_1 = 3, \quad \theta_1 = 0.7, \quad \delta_1 = 1.5. \tag{5.1}$$

First, we plot the equilibrium curve by varying fear parameter k_1 to capture the impact of fear (Fig. 2(a)). Supercritical Hopf bifurcation occurs at $k_1 = 1.9956$ (denoted by H) as first Lyapunov coefficient (l_1) is negative ($l_1 = -1.828425 \times 10^{-7}$). Saddle-node bifurcation also is found to occur for system (2.1) at $k_1 = 2.7194$ (denoted by LP). At LP, two branches of equilibrium curves collide and disappear. Continuation of limit cycles from the Hopf point has been plotted in Fig. 2(b). Stable limit cycles originate from Hopf point which further disappear at $k_1 = 1.997$, with the occurrence of Limit Point Curve (LPC). At LPC, saddle-node bifurcation of limit cycle occurs, i.e. one stable and one unstable limit cycle collide and vanish. It is evident that prey population diminishes with the increment in fear parameter. Between Hopf point $k_1 = 1.9956$ and $k_1 = 1.996$, the dynamical variables show persistent periodic oscillations. Further, between $k_1 = 1.996$ and $k_1 = 1.997$, an unstable limit cycle surrounding stable limit cycle exists. Trajectories converge to stable limit cycle only when the initial point lies inside the outer unstable limit cycle. For initial points in the exterior of the unstable limit cycle, the trajectories collapse. If $k_1 > 1.997$, then species population goes to extinction. Therefore, the prey species, which shows more anti-predator behavior, is more vulnerable to extinction.

It is obvious that for system (2.1), whenever $x(0) < A$, solution trajectories converge to the trivial equilibrium $E_0(0, 0)$. However, this is not the necessary condition, i.e. even if $x(0) > A$, the solution trajectories may move toward the trivial equilibrium depending on the initial start. In Fig. 3, we have plotted the

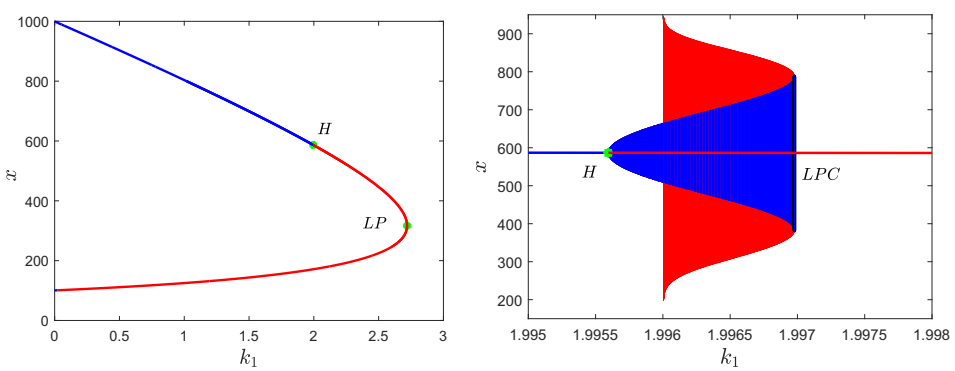

(a) (b)

Fig. 2. (Color online) (a) Equilibrium curve in x of system (2.1) with respect to k_1. Blue curve is the collection of stable co-existence equilibria and red curve is the collection of unstable co-existence equilibria. (b) Limit cycle continuation from Hopf bifurcation point. Stable limit cycles are represented by blue color and unstable limit cycles by red color.

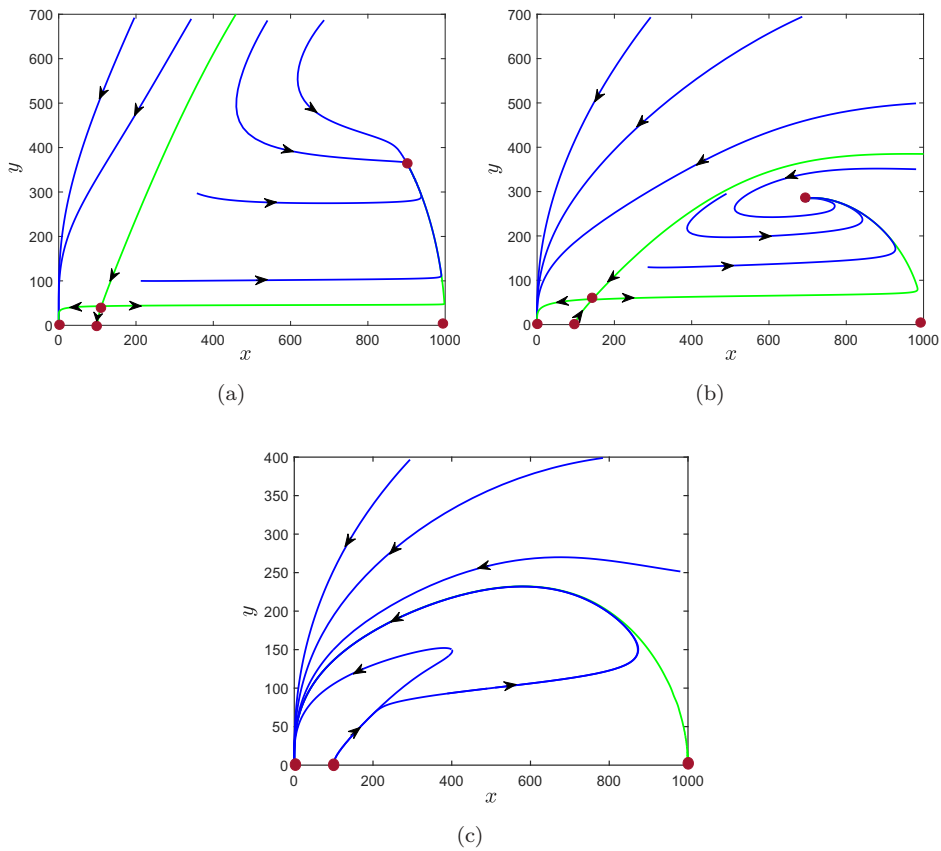

Fig. 3. Phase portraits of system (2.1) for (a) $k_1 = 0.5$, (b) $k_1 = 1.5$, and (c) $k_1 = 3$.

phase portraits for three different values of k_1. It can be clearly observed that the basin of attraction of the stable co-existence equilibrium is critically shrinking with increasing k_1. After some critical value of k_1, the co-existence equilibrium loses its stability, and then trivial equilibrium becomes globally stable. In Fig. 4, we plot x-component of equilibrium by varying the predation rate parameter α_1. The figure depicts that the system undergoes transcritical bifurcation (denoted by BP) at $\alpha_1 = 2.1428$, supercritical Hopf bifurcation at $\alpha_1 = 3.3577$ (first Lyapunov coefficient, $l_1 = -2.41598 \times 10^{-8}$) and saddle-node bifurcation at $\alpha_1 = 3.555$. For lower predation rate, the predator-free equilibrium is stable. That means predators cannot capture and arrange sufficient food to feed upon. Therefore, predator population cannot sustain in the system and as a result, the density of prey population tends to its carrying capacity. Both prey and mesopredator species co-exist for an intermediate range of predation rate α_1, depending on the initial population sizes. For higher predation rate, both the species population collapse, irrespective of initial population sizes.

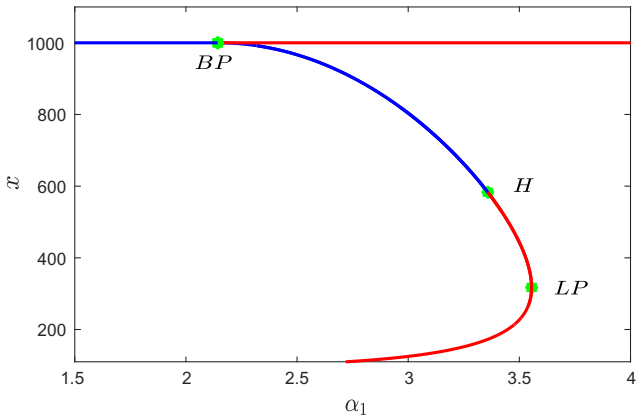

Fig. 4. (Color online) Equilibrium curve in x of system (2.1) with respect to α_1. Here, we take $k_1 = 1$. Blue curve is the collection of stable equilibria and red curve is the collection of unstable equilibria.

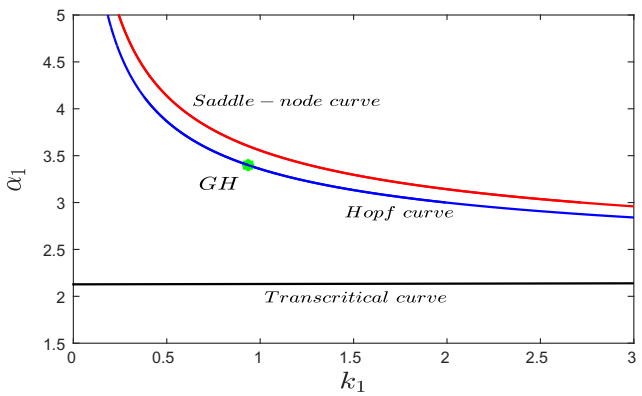

Fig. 5. Bifurcation diagram in $k_1 - \alpha_1$ parametric plane.

As we see that predation induced fear and rate of predation have the potential to modulate system's dynamics, two-parameter bifurcation diagram is plotted in $k_1 - \alpha_1$ plane (Fig. 5). Black curve denotes transcritical curve, below which co-existence equilibrium is not feasible, only mesopredator-free equilibrium is stable. In the parametric region between transcritical and Hopf curve, one stable co-existence equilibrium exists, which loses its stability as Hopf-curve is crossed. In the above saddle-node curve, co-existence equilibrium loses its feasibility again. We can infer from the figure that for less fearful prey, both the species may sustain stably in the habitat for considerably large range of predation rate. However, if the impact of fear is large enough, then higher predation rate always trigger extinction of species. Therefore, for more fearful prey, extinction is more likely to occur. Also, from Fig. 5, it is noted that if the parameter values lie in the region between transcritical curve

and Hopf curve, then the threshold value x_c determines whether the introduction of top predator should be initiated in the habitat or not. However, whenever the parameters lie above the Hopf curve, introduction of top predator is inevitable, whatsoever x_c might be.

From the above discussion, we observe that, for higher strength of fear and magnitude of predation rate, prey species equilibrium density is reducing, and even the collapse of species population is also occurring. In such a situation, the idea of introduction of top predator which predates on mesopredator but not on the considered prey species is deployed. In Fig. 6, we first plot time series for system (2.1) up to $t = 50$ unit, taking $k_1 = 1.8$ and other parameter values are same as given in Eq. (5.1). We see that system stabilizes at $(x^*, y^*) = (632.531, 253.088)$. Then at $t = 50$ unit, we introduce top predator in the system, and we plot time series from $t = 50$ unit to $t = 100$ unit, for system (2.2). The parameter values we consider for the simulations of system (2.2) are given by

$$r = 2, \quad K = 1000, \quad A = 100, \quad k_1 = 1.8, \quad \alpha_1 = 3, \quad \theta_1 = 0.7,$$
$$\delta_1 = 1.5, \quad k_2 = 0.1, \quad \alpha_2 = 0.1, \quad \theta_2 = 0.3, \quad \delta_2 = 2. \tag{5.2}$$

We observe that top predator introduction induces trophic cascading effect and system (2.2) stabilizes with very high density of prey species.

In Fig. 7, we have plotted the phase portraits of systems (2.1) and (2.2) for $k_1 = 1.8$. It is evident that the basin of attraction of the co-existence equilibrium is broadening with the incorporation of the top predator. Suppose we choose the critical value $x_c = 400$, then from Fig. 7(a), we can see that trajectories with initial start outside the basin of attraction of stable interior equilibrium, i.e. upper half of green curve, bound to cross x_c and ultimately falls to origin. The instant it crosses x_c, we will introduce top predator. With the introduction of top predator,

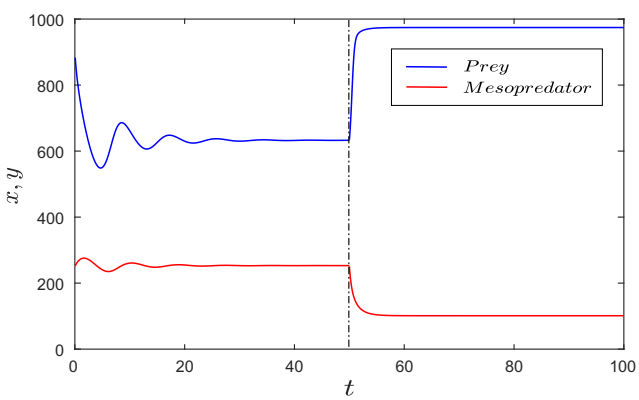

Fig. 6. (Color online) Time series of system (2.1) is plotted for time interval $[0, 50]$ and time series of system (2.2) is plotted for time interval $[50, 100]$. Here we take $k_1 = 1.8$. and other parameter values are same as given in Eq. (5.2). Blue curve represents density of prey and red curve represents the density of mesopredator.

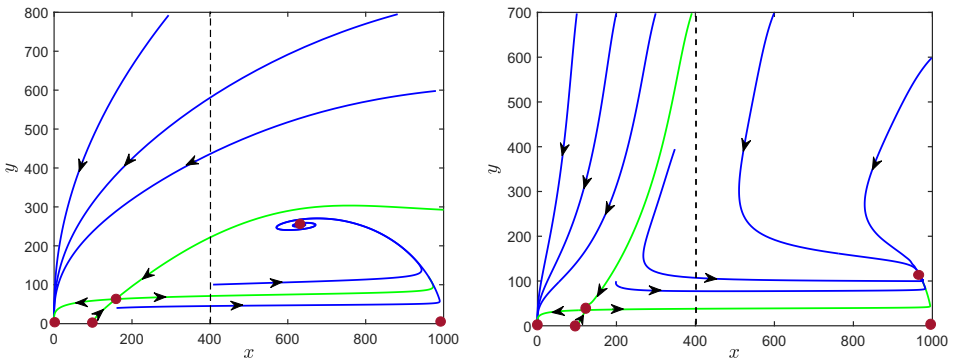

Fig. 7. Phase portraits of (a) system (2.1), and (b) system (2.2), for $k_1 = 1.8$.

the species extinction can be controlled if the solution trajectories lie inside the basin of attraction for the equilibrium of system (2.2). In Fig. 7(b), $z(0)$ is taken to be $z(0) = 5$ for all the solution trajectories, i.e. we are considering that 5 unit of top predator is being introduced. It is also observed that the value of $z(0)$ has not much influence on the basin of attraction. Even though for system (2.2) the basin of attraction of the stable co-existence equilibrium is being increased, the trajectories may also converge to origin if the initial point lie on the left of green curve (Fig. 7(b)).

Similarly, in Fig. 8, we plot time series for system (2.1) in time interval $[0, 50]$ and for system (2.2) in $[50, 100]$, taking $k_1 = 1.9965$ and other parameter values are same as given in Eq. (5.2). Figure 8 corroborates that introduction of top predator even stabilizes an oscillatory system. Also, in both the above cases, introduction

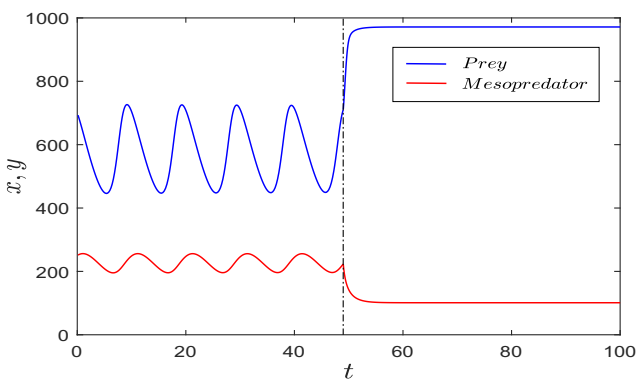

Fig. 8. (Color online) Time series of system (2.1) is plotted for time interval $[0, 50]$ and time series of system (2.2) is plotted for time interval $[50, 100]$. Here, $k_1 = 1.9965$ and other parameter values are same as given in Eq. (5.2). Blue curve represents density of prey and red curve represents the density of mesopredator.

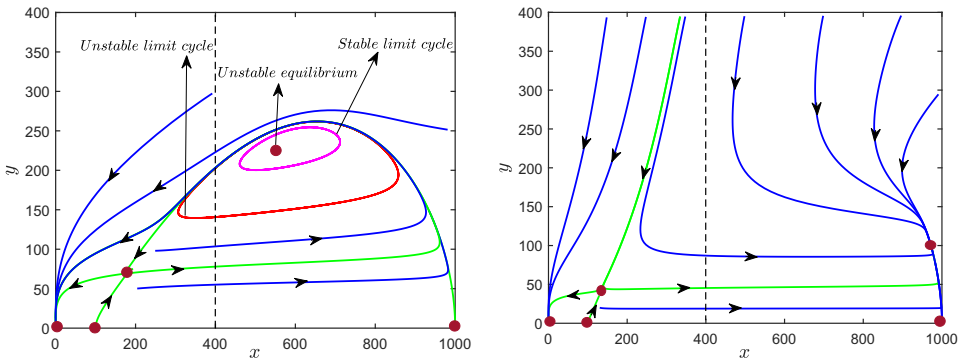

Fig. 9. Phase portraits of (a) system (2.1) and (b) system (2.2), for $k_1 = 1.9965$.

of top predator induces cascading effect. As top predator limits the density of mesopredator, the density of prey species increases.

Phase portrait of systems (2.1) and (2.2) for $k_1 = 1.9965$ is plotted in Fig. 9. One interior equilibrium of system (2.1) is saddle and the other unstable one is surrounded by a stable (magenta color) and an unstable limit cycle (green color). Region inside the unstable limit cycle serves as the basin of attraction of the stable limit cycle, which is very narrow. Otherwise the trajectories finally accumulates at origin, and in the meantime the density of prey species falls below our considered x_c. In such a situation, top predator introduction magnifies the basin of attraction of corresponding interior equilibrium many fold, mop up the oscillation, and drives the trajectories to stabilize at higher equilibrium density of prey species. Here also, some region of positive quadrant lies outside the basin of attraction of interior equilibrium, and trajectories starting in this region ultimately terminate at origin.

We have already observed in Fig. 2(a), higher strength of fear triggers population collapse. So in Fig. 10, we consider $k_1 = 2.2$ and plot times series of system (2.1) up to $t = 5$ unit, when both the species rapidly move towards extinction. Introduction of top predator at that instance mediates the system to a stable state where all the species co-exist. All trajectories in Fig. 11(a) converge to trivial equilibrium for any initial start. In such a situation, species can be prevented from extinction, provided the initial point of the trajectories of system (2.1) lies inside the basin of attraction of stable equilibrium point (Fig. 11(b)). Thus, the density of a particular species in an ecosystem can be enriched by introducing a suitable top predator. Even the extinction of a species can be avoided by timely introducing top predator.

Thereafter, we plot the equilibrium curve for system (2.2) by varying fear parameter k_1 (Fig. 12). We observe that a stable branch exists up to large value of k_1 and then the system undergoes saddle-node bifurcation at $k_1 = 14.08$, where the stable branch collides with unstable branch and co-existence equilibrium vanishes. That means when perceiving predation risk, prey species deploy most of their effort

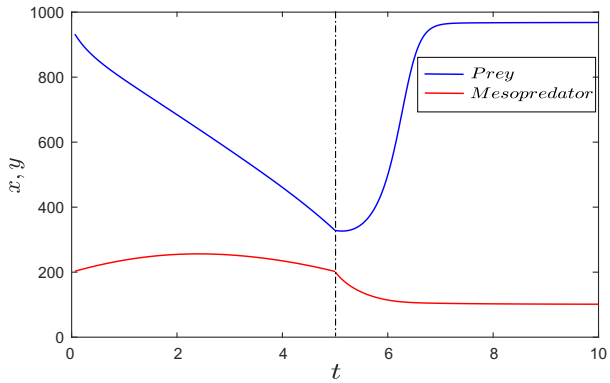

Fig. 10. (Color online) Time series of system (2.1) is plotted for time interval $[0, 5]$ and time series of system (2.2) is plotted for time interval $[5, 10]$. Here, $k_1 = 2.2$ and other parameter values are as given in Eq. (5.2). Blue curve represents density of prey and red curve represents the density of mesopredator.

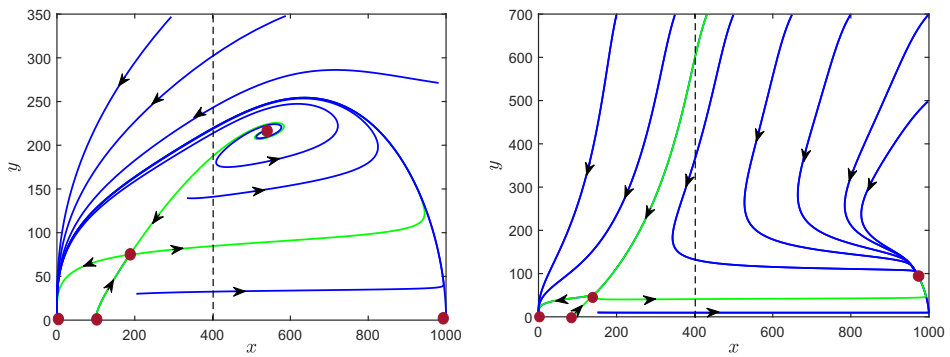

(a) (b)

Fig. 11. Phase portraits of (a) system (2.1) and (b) system (2.2), for $k_1 = 2.2$.

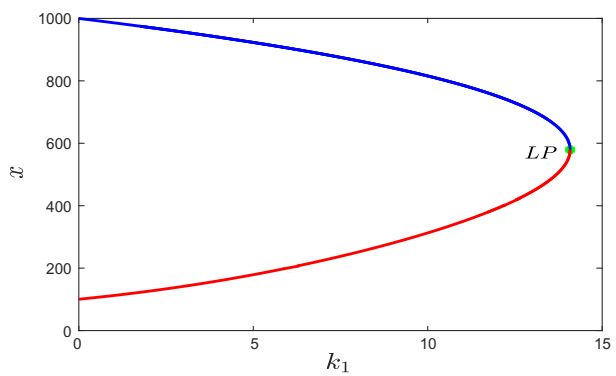

Fig. 12. (Color online) Equilibrium curve in x for system (2.2) with respect to k_1. Blue curve is the collection of stable co-existence equilibria and red curve is the collection of unstable co-existence equilibria.

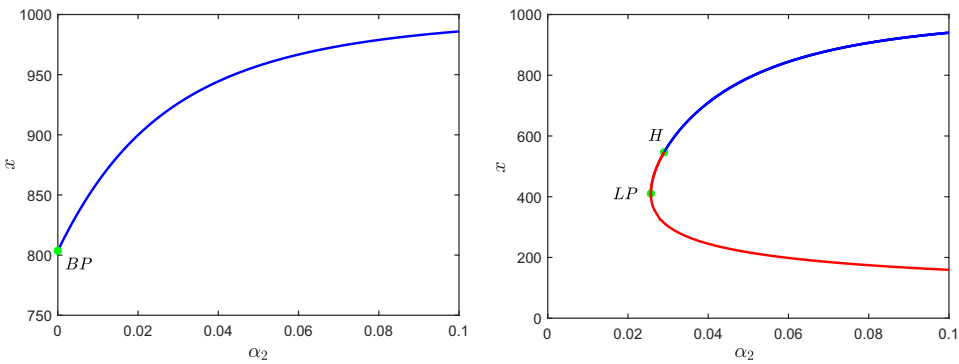

Fig. 13. (Color online) Equilibrium curve in x for system (2.2) with respect to α_2, where (a) $k_1 = 1$, (b) $k_1 = 4$. Blue curve is the collection of stable co-existence equilibria and red curve is the collection of unstable co-existence equilibria.

and time in anti-predation activities, growth rate becomes very low and prey population gradually dies out. This further implies that the whole system fall out and all the species become extinct. Figure 13(a) represents the equilibrium curve in $\alpha_2 - x$ plane, obtained by varying the predation rate of top predator (α_2), considering $k_1 = 1$ and rest of the parameter values are same as in Eq. (5.2). The system undergoes transcritical bifurcation at $\alpha_2 = 0$, and the system remains stable for all positive α_2. Keeping $\alpha_2 = 0$ is just mimicking the situation that the dynamics is governed by system (2.1), and then the system achieves its stable equilibrium $(x^*, y^*) = (803.598, 321.439)$. Now, as the top predator is introduced, and its predation rate takes any positive value, density of prey species increases from its previous state. However, for $k_1 = 4$, the system shows different kinds of dynamics (Fig. 13(b)). System (2.2) remains stable for relatively higher values of α_2. It undergoes Hopf bifurcation at $\alpha_2 = 0.029$, which is subcritical in nature ($l_1 = 4.734 \times 10^{-6}$), and saddle-node bifurcation at $\alpha_2 = 0.0257$. Therefore, the system experiences population collapse or species extinction if α_2 decreases below 0.029. Since we consider $k_1 = 4$, we can see from Fig. 2(a) that system (2.1) already experiencing population collapse. Therefore, top predator is introduced at some instance of time to re-instate the species. However, if the top predators are found to be weak, failed to capture mesopredator at some considerable rate, then the target of enriching x-species population cannot be achieved.

Furthermore, to get more intriguing effect of k_1 and α_2 on the dynamics of system (2.2), we plot bifurcation diagram in $k_1 - \alpha_2$ parametric plane (Fig. 14). The red, blue and black color curve, respectively, representing the saddle-node, Hopf and homoclinic curve, all of which converge to BT-bifurcation point. Below the saddle- node curve, the system has no co-existence equilibrium. Between saddle-node and Hopf curve, although two co-existence equilibria exist, both are unstable. Between Hopf and homoclinic curve, one co-existence equilibrium gains stability

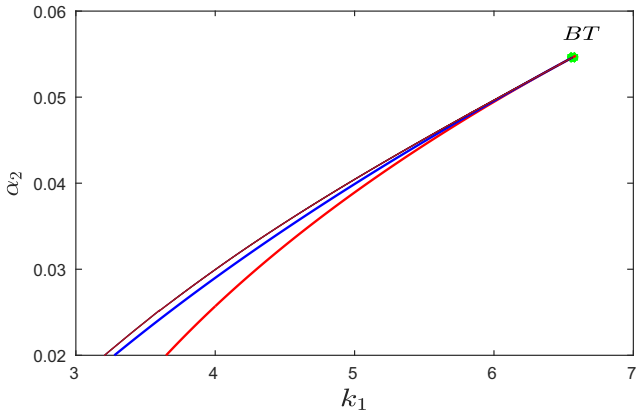

Fig. 14. (Color online) Bifurcation diagram of system (2.2) in $k_1 - \alpha_2$ parametric plane. Rest parameter values are same as given in (5.2). The red, blue and black color curves, respectively, representing the saddle-node, Hopf and homoclinic curve.

through Hopf bifurcation with an unstable limit cycle surrounding the equilibrium. In such case, if the initial point lies in the interior of unstable limit cycle, then trajectories converge to the stable co-existence equilibria, otherwise the trajectories fall out. Above the homoclinic curve, the unstable limit cycle vanishes with the occurrence of homoclinic bifurcation and the system has only a stable and an unstable co-existence equilibria. Biologically, the figure interprets that if the prey species is more fearful and show strong anti-predation behavior, then in order to protect ecosystem from collapsing, predation rate of introduced top predator should be high enough.

Now, to understand the combining impact of both fear parameters on the density of targeted species (prey) population, we draw equilibrium curve of system (2.2) with respect to fear parameter k_2, for three different values k_1, represented by Fig. 15. The complete dynamics of system (2.2) with respect to k_1 and k_2 is captured in Fig. 16. Similar kind of dynamics as explained for Fig. 14 is observed in this case also. When the strength of mesopredator induced fear on prey population is weak, density of prey population maintained at higher level, whatever the strength of top predator induced fear might be. However, if the cost of fear on prey population is relatively high, then the strength of top predator induced fear should be comparatively high for the stable co-existence of the species in the system. Parameters should lie above the black curve (homoclinic curve) for stable co-existence of all the species with density of prey population at higher level. Therefore, if the targeted species is less responsive toward mesopredator induced fear, the purpose of elevating prey density would be successful by the introduction of top predator. However, for more fearful prey species, the motive can be achieved if the strength of top predator induced fear on mesopredator is comparatively higher.

Although increasing mesopredator induced fear factor (k_1) leads to shrinking of basin of attraction of the stable equilibrium of system (2.2), but increase in

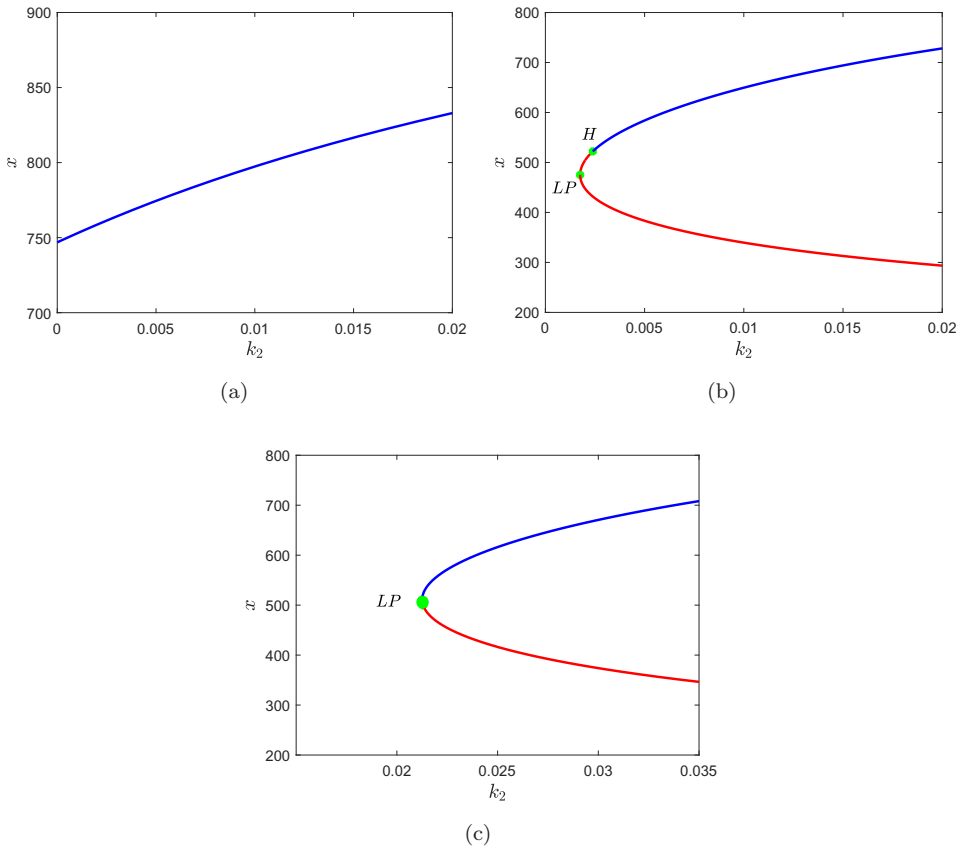

Fig. 15. (Color online) Equilibrium curve of system (2.2) with respect to k_2, where (a) $k_1 = 4$, (b) $k_1 = 5.6$, (c) $k_1 = 7$. Blue curve is the collection of stable co-existence equilibria and red curve is the collection of unstable co-existence equilibria.

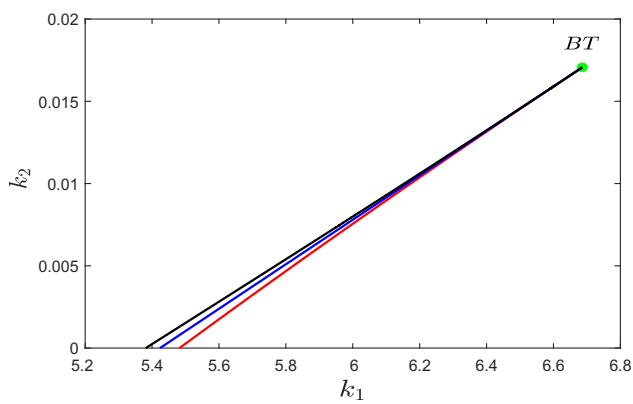

Fig. 16. (Color online) Bifurcation diagram of system (2.2) in $k_1 - k_2$ parametric plane. Rest parameter values are same as given in Eq. (5.2). The red, blue and black color curves, respectively, representing the saddle-node, Hopf and homoclinic curve.

predation rate (α_2) and top predator induced fear (k_2) has a positive impact in expanding the basin of attraction.

6. Conclusion

Over the course of time, many species have gone extinct and a large number of species have been declared endangered. Sometimes, the species population in a habitat becomes low due to over-predation augmented with some environmental factors. Previously, the producers and the herbivores are believed to be main contributors in shaping an ecosystem and the ecologists conceived the concept of bottom-up approach that governs an ecosystem. With experimental evidences collected from various ecosystem, ecologists started to understand that an ecosystem is not totally controlled by the producers or primary consumers, those occupying the lower trophic level. The tertiary consumers or apex predators, those comprise the higher trophic levels of a food chain are also important drivers of ecosystem. From the inception of *Green World Hypothesis* by Hairston *et al.* [20], the idea of top-down mechanism surfaced in the scientific community. From thereon, the role of predator in maintaining a healthy ecosystem is being studied more and more. In this study, we theoretically conceptualize the role of top predator in protecting a prey species from extinction, in presence of mesopredator. The main idea is that if the targeted species (prey) population in the considered habitat falls below a certain threshold, top predator would be introduced in that habitat. We can call it as species population enrichment in a habitat. For the proposed mathematical model, feasibility conditions of interior equilibrium and its stability conditions are obtained. Following are the results of our study obtained theoretically and numerically:

(1) For system (2.1), in the absence of top predator, the density of prey species is always decreasing with the increasing strength of fear and predation rate. Also, the basin of attraction of the stable co-existence equilibrium is observed to be shrinking critically with increasing fear parameter and predation rate.
(2) Beyond certain threshold value of fear parameter or predation rate, population collapse and both species extinct.
(3) Our theoretical study suggests that the elevation of density of lower trophic species in the considered region can be possible with the introduction of a top predator, which feed upon the mesopredator only but not on prey.
(4) Also top predator introduction can eliminate the persistent periodic oscillation of species density and drive the system to stable state.
(5) More importantly, species extinction can be prevented by timely introduction of top predator in the habitat.
(6) If the impact of predation induced fear is very high on prey species, then in order to reinstate the density of prey species at higher level either the predation rate of top predator should be relatively high or the effect of fear on mesopredator is strong enough.

Acknowledgments

Authors sincerely thank anonymous reviewers and the editor for their fruitful comments. Soumitra Pal is thankful to the Council of Scientific and Industrial Research (CSIR), Government of India for providing financial support in the form of senior research fellowship (File No. 09/013(0915)/2019-EMR-I).

ORCID

A. K. Misra https://orcid.org/0000-0002-2885-9955
Soumitra Pal https://orcid.org/0009-0007-6554-1149
Yun Kang https://orcid.org/0000-0001-5448-7609

References

[1] Animal and plant species declared extinct between 2010 and 2019, the full list, https://www.lifegate.com/extinct-species-list-decade-2010-2019.
[2] IUCN, The IUCN Red List of Threatened Species, Version 2019-2 (IUCN, 2019), http://www.iucnredlist.org
[3] P. Aguirre, J. D. Flores and E. Gonzalez-Olivares, Bifurcations and global dynamics in a predator–prey model with a strong Allee effect on the prey, and a ratio-dependent functional response, *Nonlinear Anal. Real world Appl.* **16** (2014) 235–249.
[4] M. C. Allen, M. Clinchy and L. Y. Zanette, Fear of predators in free-living wildlife reduces population growth over generations, *Proc. Natl. Acad. Sci.* **119**(7) (2022) e2112404119.
[5] R. Arditi and L. R. Ginzburg, Coupling in predator–prey dynamics: Ratio–dependence, *J. Theor. Biol.* **139** (1989) 311–326.
[6] R. Arditi, L. R. Ginzburg and H. R. Akcakaya, Variation in plankton densities among lakes: a case for ratio-dependent models, *Am. Nat.* **138** (1991) 1287–1296.
[7] T. B. Atwood, S. A. Valentine, E. Hammill, D. J. McCauley, E. M.P. Madin, K. H. Beard and W. D. Pearse, Herbivores at the highest risk of extinction among mammals, birds, and reptiles, *Sci. Adv.* **6**(32) (2020) eabb8458.
[8] C. M. Baker, A. Gordon and M. Bode, Ensemble ecosystem modeling for predicting ecosystem response to predator reintroduction, *Conserv. Biol.* **31**(2) (2017) 376–384.
[9] M. J. Bishop, B. P. Kelaher, M. Smith, P. H. York and D. J. Booth, Ratio-dependent response of a temperate Australian estuarine system to sustained nitrogen loading, *Oecologia* **149** (2006) 701–708.
[10] L. Cheng and H. Cao, Bifurcation analysis of a discrete–time ratio–dependent predator–prey model with Allee effect, *Commun. Nonlinear Sci. Numer. Simul.* **38** (2016) 288–302.
[11] M. Clinchy, M. J. Sheriff and L. Y. Zanette, Predator–induced stress and the ecology of fear, *Funct. Ecol.* **27**(1) (2013) 56-65.
[12] P. Cong, M. Feng and X. Zou, Dynamics of a three-species food chain model with fear effect, *Commun. Nonlinear Sci. Numer. Simul.* **99** (2021) 105809.
[13] C. Conser, D. L. Angelis, J. S. Ault and D. B. Olson, Effects of spatial grouping on the functional response of predators, *Theor. Popul. Biol.* **56** (1991) 65–75.
[14] K. H. Elliot, G. S. Betini and D. R. Norris, Fear creates an Allee effect: Experimental evidence from seasonal populations, *Proc. R. Soc. B, Biol. Sci.* **284**(1857) (2017) 20170878.

[15] J. D. Flores and E. Gonzalez-Olivares, Dynamics of a predator–prey model with Allee effect on prey and ratio-dependent functional response, *Ecol. Complex.* **18** (2014) 59–66.
[16] Y. Gao and B. Li, Dynamics of a ratio-dependent predator–prey system with a strong Allee effect, *Discr. Contin. Dynam. Syst. B* **18**(9) (2013) 2283.
[17] C. E. Gordon, A. Feit, J. Gruber and M. Lentic, Mesopredator suppression by an apex predator alleviates the risk of predation perceived by small prey, *Proc. R. Soc. B* **282** (2015) 20142870.
[18] A. Gupta, A. Kumar and B. Dubey, Complex dynamics of Leslie–Gower prey–predator model with fear, refuge and additional food under multiple delays, *Int. J. Biomath.* **15**(08) (2022) 2250060.
[19] A. P. Gutirrez, The physiological basis of ratio-dependent predator–prey theory: A metabolic pool model of Nicholsons blowflies as an example, *Ecology* **73** (1992) 1552–1563.
[20] N. G. Hairston, F. E. Smith and L. B. Slobodkin, Community structure, population control and completion, *Am. Nat.* **94**(879) (1960) 421–425.
[21] M. Haque, Ratio-dependent predator–prey models of interacting populations, *Bull. Math. Biol.* **71** (2009) 430–452.
[22] M. D. Hooper, The size and surroundings of nature reserves, in *The Scientific Management of Animal and Plant Communites for Conservation* (Blackwell Oxford, 1971), pp. 555–561.
[23] S. Hsu, T. Hwang and Y. Kuang, Global analysis of the Michaelis–Menten type ratio-dependent predator–prey system, *J. Math. Biol.* **42** (2001) 489–506.
[24] S. Hsu, T. Hwang and Y. Kuang, Rich dynamics of a ratio-dependent one-prey two-predators model, *J. Math. Biol.* **43** (2001) 377–396.
[25] S. Hsu, T. Hwang and Y. Kuang, A ratio-dependent food chain model and its application, *Math. Biosci.* **181** (2003) 55–83.
[26] Y. Kang and O. Udiani, Dynamics of a single species evolutionary model with Allee effects, *J. Math. Anal. Appl.* **418** (2014) 492–515.
[27] Y. Kuang and E. Beretta, Global qualitative analysis of a ratio-dependent predator–prey system, *J. Math. Biol.* **36** (1998) 389–406.
[28] A. Kumar and B. Dubey, Modeling the effect of fear in a prey–predator system with prey refuge and gestation delay, *Int. J. Bifurc. Chaos* **29**(14) (2019) 1950195.
[29] Y. A. Kuznetsov, *Elements of Applied Bifurcation Theory*, Vol. 112 (Springer Science and Business Media, NY, 2013).
[30] A. J. Lotka, *Elements of Physical Biology* (Williams and Wilkins Company, Baltimore, 1925).
[31] E. Numfor, F. M. Hilker and S. Lenhart, Optimal culling biocontrol in a predator–prey model, *Bull. Math. Biol.* **79** (2017) 88–116.
[32] N. M. Oliveira and F. M. Hilker, Modelling disease introduction as biological control of invasive predators to preserve endangered species, *Bull. Math. Biol.* **72** (2010) 444–468.
[33] S. Pal, A. Gupta, A. K. Misra and B. Dubey, Complex dynamics of a predator–prey system with fear and memory in the presence of two discrete delays, *Eur. Phys. J. Plus* **138** (2023) 984.
[34] S. Pal, P. K. Tiwari, A. K. Misra and H. Wang, Fear effect in a three-species food chain model with generalist predator, *Math. Biosci. Eng.* **21**(1) (2024) 1–33.
[35] S. Pal, P. Panday, N. Pal, A. K. Misra and J. Chattopadhyay, Dynamical behaviors of a constant prey refuge ratio–dependent prey–predator model with Allee and fear effects, *Int. J. Biomath.* **17**(1) (2023) 2350010.

[36] P. Panday, N. Pal, S. Samanta and J. Chattopadhyay, A three species food chain model with fear induced trophic cascade, *Int. J. Appl. Comput. Math.* **5**(100) (2019) 1–26.
[37] L. Perko, *Differential Equation and Dynamical System* (Springer, New York, 2001).
[38] M. E. Power, Top-down and bottom-up forces in food webs: Do plants have primacy? *Ecology* **73**(3) (1992) 733–746.
[39] W. J. Ripple and R. L. Beschta, Trophic cascades in Yellowstone: The first 15 years after wolf reintroduction, *Biol. Conserv.* **145**(1) (2012) 205–213.
[40] K. Sarkar and S. Khajanchi, Impact of fear on the growth of prey in a predator–prey interaction model, *Ecol. Complex.* **42** (2020) 100826.
[41] S. K. Sasmal, Population dynamics with multiple Allee effects induced by fear factors: a mathematical study on prey–predator interactions, *Appl. Math. Model.* **64** (2018) 1–14.
[42] S. K. Sasmal and Y. Takeuchi, Modeling the Allee effects induced by cost of predation fear and its carry-over effects, *J. Math. Anal. Appl.* **505** (2022) 125485.
[43] M. Sen, M. Banerjee and A. Morozov, Bifurcation analysis of a ratio-dependent prey–predator model with the Allee effect, *Ecol. Complex.* **11** (2012) 12–27.
[44] F. Sergio, T. Caro, D. Brown, B. Clucus, J. Hunter, J. Ketchum, K. McHugh and F. Hiraldo, Top predators as conservation tools: Ecological rationale, assumptions, and efficacy, *Annu. Rev. Ecol. Evol. Syst.* **39** (2008) 1–19.
[45] M. L. Shaffer, Minimum population size for species conservation, *Bioscience* **31**(2) (1981) 131–134.
[46] M. J. Sheriff, C. J. Krebs and R. Boonstra, The sensitive hare: Sublethal effects of predator stress on reproduction in snowshoe hares, *J. Anim. Ecol.* **78**(6) (2009) 1249–1258.
[47] M. J. Sheriff, S. D. Peacor, D. Hawlena and M. Thaker, Non-consumptive predator effects on prey population size: A dearth of evidence, *J. Anim. Ecol.* **89**(6) (2020) 1302–1316.
[48] D. W. Smith and R. O. Peterson, Intended and unintended consequences of wolf restoration to Yellowstone and Isle Royale National Parks, *Conserv. Sci. Pract.* **3**(4) (2021) e413.
[49] J. P. Suraci, M. Clinchy, L. M. Dill, D. Roberts and L. Y. Zanette, Fear of large carnivores causes a trophic cascade, *Nat. Commun.* **7** (2016) 10698.
[50] V. Tiwari, J. P. Tripathi, S. Mishra and R. K. Upadhyay, Modeling the fear effect and stability of non-equilibrium patterns in mutually interfering predator–prey systems, *Appl. Math. Comput.* **371** (2020) 124948.
[51] P. K. Tiwari, M. Verma, S. Pal, Y. Kang and A. K. Misra, A delay nonautonomous predator–prey model for the effects of fear, refuge and hunting cooperation, *J. Biol. Syst.* **29**(04) (2020) 927–969.
[52] H. Verma, K. Antwi-Fordjour, M. Hossain, N. Pal, R. D. Parshad and P. Mathur, A double fear effect in a tri-trophic food chain model, *Eur. Phys. J. Plus.* **136**(905) (2021) 1–17.
[53] M. Verma and A. K. Misra, Modeling the effect of prey refuge on a ratio-dependent predator–prey system with the Allee effect, *Bull. Math. Biol.* **80**(3) (2018) 626–656.
[54] V. Volterra, Variations and fluctuations of the number of individuals in animal species living together, *Memorie della R. Accademia Nazionale dei Lincei* **2** (1926) 31–113.
[55] J. Wang, J. Shi and J. Wei, Predator–prey system with strong Allee effect in prey, *J. Math. Biol.* **62**(3) (2011) 291–331.

[56] W. Wang, Y. Zhu, Y. Cai and W. Wang, Dynamical complexity induced by Allee effect in a predator–prey model, *Nonlinear Anal. Real World Appl.* **16** (2014) 103–119.
[57] X. Wang, L. Zanette and X. Zou, Modelling the fear effect in predator–prey interactions, *J. Math. Biol.* **73**(5) (2016) 1179–1204.
[58] D. Xiao and S. Ruan, Global dynamics of a ratio-dependent predator–prey system, *J. Math. Biol.* **43**(3) (2001) 268–290.
[59] L. Y. Zanette, A. F. White, M. C. Allen and M. Clinchy, Perceived predation risk reduces the number of offspring songbirds produce per year, *Science* **334** (2011) 1398–1401.
[60] X. Zeng, W. Zeng and L. Liu, Effect of the protection zone on coexistence of the species for a ratio–dependent predator–prey model, *J. Math. Anal. Appl.* **462** (2018) 1605–1626.
[61] H. Zhang, Y. Cai, S. Fu and W. Wang, Impact of the fear effect in a prey–predator model incorporating a prey refuge, *Appl. Math. Comput.* **356** (2019) 328–337.
[62] S. Zhou, Y. Liu and G. Wang, The stability of predator–prey systems subject to the Allee effects, *Theor. Popul. Biol.* **67**(1) (2005) 23–31.
[63] J. Zu and M. Mimura, The impact of Allee effect on a predator–prey system with Holling type II functional response, *Appl. Math. Comput.* **217**(7) (2010) 3542–3556.